T.R.

KAHRAMANMARAŞ SÜTÇÜ İMAM UNIVERSITY

GRADUATE SCHOOL OF NATURAL AND APPLIED SCIENCES

DETERMINING THE IMPACT OF URBAN EXPANSION ON LAND SURFACE TEMPERATURE IN ADANA-TURKEY

SORAN OMAR AHMED

MASTER'S THESIS

DEPARTMENT OF BIOENGINEERING AND SCIENCES

KAHRAMANMARAŞ - TURKEY 2015

T.R.
KAHRAMANMARAŞ SÜTÇÜ İMAM UNIVERSITY
GRADUATE SCHOOL OF NATURAL AND APPLIED SCIENCES

DETERMINING THE IMPACT OF URBAN EXPANSION ON LAND SURFACE TEMPERATURE IN ADANA-TURKEY

SORAN OMAR AHMED

A thesis submitted in partial fulfillment of the requirements for the degree of Master of Science in Bioengineering and Sciences

KAHRAMANMARAŞ - TURKEY 2015

M.Sc. thesis entitled “Determining the Impact of Urban Expansion on Land Surface Temperature in Adana-Turkey” and prepared by Soran Omar AHMED, who is a student at Department of Bioengineering and Sciences, Graduate School of Natural and Applied Sciences, Kahramanmaraş Sütçü İmam University, was certified by all the majority jury members, whose signatures are given below at the date of 29/6/2015

Assist. Prof. Hakan OĞUZ (Supervisor) …….
Department of Landscape Architecture
Kahramanmaraş Sütçü İmam University

Assoc. Prof. Murat KARABULUT (Member) …….
Department of Geography
Kahramanmaraş Sütçü İmam University

Assoc. Prof. Hasan SERIN (Member) …….
Department of Forest Industry Engineering
Kahramanmaraş Sütçü İmam University

I approve that the above signatures related to the members.

Assoc. Prof. MUSTAFA ŞEKKELİ …….
Director of Graduate School

DECLARATION

I declare and guarantee that all information in this document has been obtained and presented in accordance with academic rules and ethical conduct. Based on these rules and conduct, I have fully cited and referenced all material and results that are not original to this work.

SORAN OMAR AHMED

ADANA KENT BÜYÜMESININ YER YÜZEY SICAKLIĞI ÜZERİNE ETKİSİNİN BELİRLENMESİ

(YÜKSEK LİSANS TEZİ)

SORAN OMAR AHMED

ÖZET

Son yıllarda, küresel ısınma, sera etkisi ve diğer birçok çevre problemleri çözümlenmesi gereken en popüler konular olmuştur. Yer yüzey sıcaklığı (YYS) birçok çevre modelleri için önemli bir parametredir. Kent büyümesi doğal peyzajı antropojenik kent yapısına dönüştürmekte ve kentteki yüzeye ait fiziksel karakteristikleri değiştirmede önemli rol oynamaktadır. Bu etkilerden bir tanesi ise yüzey sıcaklığı değişimi olup yerel hava durumu üzerinde önemli etkileri bulunmaktadır. Bu çalışmanın amacı Adana da ki mekânsal kent büyümesinin yer yüzey sıcaklığı üzerine etkisinin incelenmesi oluşturmaktadır.

Bu çalışmada, uzaktan algılama (UA) ve coğrafi bilgi sistemleri (CBS) teknikleri kullanılarak önce arazi kullanımı / arazi örtüsü (AK/AÖ) değişimi tespit edilmiş daha sonra ise bu değişimin yer yüzey sıcaklığı üzerine etkileri belirlenmiştir. AK/AÖ değişimi ise 1991 ve 2011 yaz aylarına ait Landsat 5 uydu görüntülerinden elde edilmiştir. YYS verilerini Landsat uydu görüntülerinden elde etmek Oguz H. (2013) tarafından geliştirilen "LST Calculator" isimli bir bilgisayar programından yararlanılmıştır.

Bulgular göstermiştir ki Adana da ki yer yüzey sıcaklığı değişimlerinin en büyük etmeni kentsel dokunun aşırı büyümesidir. Yer yüzey sıcaklığı dağılımının mekânsal deseni ile kent büyüme deseni arasında doğru orantılı; yer yüzey sıcaklığı ile vejetasyon yoğunluğu arasında ise ters orantılı bir ilişkinin olduğu tespit edilmiştir.

Sonuç olarak, uzaktan algılama ve coğrafi bilgi sistemleri teknolojileri kent büyüme desenlerinin ve onların yer yüzey sıcaklığı üzerine etkilerinin izlenmesinde ve analiz edilmesinde etkili olmuştur.

Anahtar Kelimeler: AK/AÖ Değişimi, Kentleşme, Yer Yüzey Sıcaklığı, NDVI, UA, CBS

Kahramanmaraş Sütçü İmam Üniversitesi

Fen Bilimleri Enstitüsü

Biyomühendislik ve Bilimleri Anabilim Dalı, Haziran / 2015

Danışman: Yrd. Doc. Dr. Hakan OĞUZ

Sayfa sayısı: 53

DETRMINING THE IMPACT OF URBAN EXPANSION ON LAND SURFACE TEMPERATURE IN ADANA-TURKEY

(M.Sc. THESIS)

SORAN OMAR AHMED

ABSTRACT

In the last decades, global warming, enhanced green-house effects and other environmental problems have become very popular subjects to overcome. Land surface temperature (LST) is an important parameter for many environmental models. Urban expansion transforms the natural landscape to anthropogenic urban land and plays important role in changing surface physical characteristics. One of these effects is surface temperature variation that might have significant effects on local weather. The main objective of this study was to investigate the effects of urban expansion on surface temperature of Adana - Turkey.

In this study, remote sensing (RS) and geographical information systems (GIS) techniques were used to detect the land use/land cover (LU/LC) change and its impact on land surface temperature. LU/LC maps of two different dates were derived from Landsat 5 Thematic Mapper (TM) images of 1991 and 2011. In order to retrieve LST from Landsat 5 TM images, a computer program, LST Calculator, developed by Oguz H. (2013) has been employed.

The results revealed that urban expansion was the major factor for the changes in land surface temperature. The spatial pattern of surface temperature distribution was correlated with the pattern of urban expansion. The increase of land surface temperature was inversely correlated to the decrease of NDVI (Normalized Difference Vegetation Index).

Overall, remote sensing and geographic information system technologies were effective approaches for monitoring and analyzing urban growth patterns and evaluating their impacts on land surface temperature.

Key words: LU/LC Change, Urbanization, Land Surface Temperature, NDVI, RS, GIS

Kahramanmaras Sutcu Imam University

Graduate School of Natural and Applied Sciences

Department of Bioengineering and Sciences, June / 2015

Supervisor: Assist. Prof. Hakan OĞUZ

Page number: 53

ACKNOWLEDGEMENTS

First of all, I would like to thank God, the almighty, for having made everything possible by giving me strength and courage to finish this thesis.

I am so grateful to my supervisor Assist. Prof. Hakan OĞUZ for his guidance, support and advice during this research. I would like to thank him for taking his valuable time to do the calculations and maps, and go through everything I wrote and offering me the numerous suggestions. Also, I would like to thank Assoc. Prof. Murat KARABULUT and Assoc. Prof. Hasan SERIN, for evaluating my thesis and for their constructive comments and suggestions.

Honestly, this thesis would not have been completed without the help of Dr. Abdulla H. A. Bilbas. I would like to thank him for helping me. Also, I am very much grateful to Ms. Suhaila ZANDY, whose encouragement helped me during the translation of this thesis.

My sincere gratitude goes towards my family for their support and interest. I also would like to thank my friends from Kurdistan for making the time spent memorable.

Finally, I would like to thank all who contributed in any way in making this research possible.

SORAN OMAR AHMED

TABLE OF CONTENTS

Pages No

LIST OF FIGURES

Pages No

LIST OF TABLES

Pages No

LIST OF ABBREVIATION

DA : Dual Angle
DN : Digital Number
ESRI : Environmental Systems Research Institute
ET : Evaporate Transpiration
ETM+ : Enhanced Thematic Mapper Plus
GHSL : Global Human Settlement Layer
GIS : Geographic Information System
ha : Hectares
ISA : Impervious Surface Area
JRC : Joint Research Centre
LST : Land Surface Temperature
LU/LC : Land use and Land cover
MLA : Maximum Likelihood Algorithm
MSS : Multispectral Scanner Sensor
NDVI : Normalize Deference Vegetation Index
NDVITHM : Normalize Deference Vegetation Index Thresholds Method
NIC : Newly Industrialized Countries
OBIA : Object Based Image Analysis
RMSD : Root Mean Square Deviation
RS : Remote Sensing
RTE : Radiative Transfer Equation
SC : Single Chanel
SW : Split Window
TES : Temperature and Emissivity Separation
TM : Thematic Mapper
TOA : Top of the Atmosphere
UHI : Urban Heat Island
UNFPA : United Nations Fund for Population Activities
UNNGLS : United Nations Non-Governmental Liaison Service
USGS : United State Geological Survey

1. INTRODUCTION

1.1. Background

Earth system is a complicated cycle with a lot of interconnected components like The Earth's surface, and it's interior. The earth surface is naturally covered by different land cover types that are mainly distributed based on climate patterns. Adding increasing human population and his needs to this balanced system. We will find lots of disturbances stem from the concept of how we change the use of the land to face our needs and regardless to its capacity or environmental impacts (Youneszadeh, 2013).

Urbanization takes places in significantly various forms. In any specific city, new urbanization can be conducted with the same density (people per km2) as those which prevailed existing built - up areas, with increased density or with low density. In fill over the remaining open space in built - up areas, or through development of new greenfield in non - urban areas in previous use. That encroach on wetlands, watersheds, forests, and other sensitive environments that require protection, as well as on farms and fields and orchards surrounding the city. (Angel et al 2005).

Urbanization is one of the most significant phenomena of the anthropogenic influence on the Earth's environment (Bobrinskaya, 2012). It is also, (Luck and Wu, 2002) reckons that It can be said that urbanization is probably the most dramatic form of land conversion , which fundamentally affect biodiversity and human life. However, more concise urbanization known physical growth of urban areas as a result of migration from rural areas and suburbs even concentrated in cities, especially larger too.

As well as, (Alig and Healy, 1987) says that, Natural and human environmental activities such as fire, agriculture, and deforestation have profound impacts upon global systems. While the Human induced land conversion the most striking current era of urbanization.On global scale, is the Urbanization process of converting from natural to artificial land cover featuring human settlements, workplaces, and other infrastructure such as roads. A complete definition of urbanization can be described as a massive unplanned global experiment affecting increasingly large acreages of the Earth's surface.

Urbanization is one of the major social and scientific changes spreading around the globe at an explosive pace, especially in developing countries. Soon, a majority of the world's people will be living in urban environments quite unlike the rural settings that have been home to most of the human society to date. The ability of human species to manage this phenomenon and also preserve the environment both globally and locally is in serious doubt. One important aspect of the environmental issues of urbanization that requires clear understanding is the change in the climate of the area being considered. The expected future consequences of urban climate change also need to be addressed for the developing countries (Tayanc and Toros, 1997).

At the same time (Weng, 2001) mentions that, Urbanization, the conversion of other types of land to uses associated with growth of populations and economy, is a main type of land use and land cover change in human history. It has a great impact on climate. By covering with buildings, roads and other impervious surfaces, urban areas generally have higher solar radiation absorption, and a greater thermal capacity and conductivity. Thus, that heat is stored during the day and released at night.

According to the Population Census of 2000, The Republic of Turkey, as one of the NIC's (Newly Industrialized Countries), has population of 67.8 million, a 65% urbanization level. In the early 1950 s, began rural-to-urban migration and urbanization are widespread. During the period between 1950 and 2000, the 1980 can be considered as one of the most important turning points. The natural population growth rate decreased from 2.4-2.8 per cent to 2.1 per cent. For the first time, the rural population began to decline. Liberal economy has confirmed, international trade, export sector based on industrial goods manufacturer, and the financial sector. Another striking features of suburbanization and urbanization in the past started to take place, and inflows of urban areas to urban areas far exceeded the flows of rural to urban areas (Gedik, 2003).

Moreover, Tunga *et al.* (2012) revealed that the turkey has made the transition to a highly urbanized country. It needed to develop appropriate institutions and regulatory frameworks to deal with the challenge sand requirements of rapid urbanization. Some issues have been adequately dealt with (e.g. provision of basic services to new dwellers), some still require institutional responses. Some specific applications are considered on the priority policy areas of interest to the Government of Turkey. (city competitiveness, urban transport, Land and housing, municipal finance).

1.2. Global Urban Expansion and Population

The urbanization process has historically been associated with other important economic and social transformations, which brought more geographical mobility and low fertility rate and longer life expectancy and an aging population. Cities important programmes for development and poverty reduction in both urban and rural, as it focuses a great deal of national economic activity, Government, trade, transport, and provide crucial links with rural areas between cities and across international borders. Often associated with urban living with higher levels of literacy and education, improve health and increase access to social services, and strengthen the cultural, political participation. (United Nations, 2014).

The world is undergoing the largest wave of urban growth in its history. The 3 billion populations of towns and cities in 2005 will increase by 1.8 billion by 2030. The fastest growth will be in the poorer urban areas. For example, the slum population of Dhaka has more than doubled in a decade, from 1.5 million in 1996 to 3.4 million in 2006. Most urban growth comes from natural increase (more births than deaths) (Martine and Marshall, 2007). Between 2000 and 2030, Asia's urban population will increase from 1.36 billion to 2.64 billion (UN NGLS 2013).

In 2008 for the first time population of more than half of the world will live in urban areas. By 2030, towns and cities will be home to approximately 5 billion people. Will double the urban population in Africa and Asia in less than a generation. This change unprecedented could enhance development and promote sustainability, or could deepen poverty and accelerate environmental degradation. The report summarizes the State of world population 2007 challenges and opportunities ahead, and the inevitability of urban growth. It also dispels many misconceptions about urbanization and calls on policymakers to take coordinated and proactive steps to harness the potential of cities to improve the lives of all. (UNFPA 2007).

At the same time Angel *et al.* (2005) mentions that, if average densities continue to decline at the annual rate of 1.7%, as they have during the past decade, the built-up area of developing-country cities will increase to more than 600,000 square kilometers by 2030. In other words, by 2030 these sities can be expected to triple their land area, with every new resident converting, on average, some 160 square meters of non-urban to urban land during the coming years.

Globally, more people live in urban areas than in rural areas. In 2007, for the first time in history, the global urban population exceeded the global rural population. In 1950, more than two-thirds (70 percent) of people worldwide lived in rural settlements and less than one-third (30 per cent) in urban settlements. In 2014, 54 percent of the world's population is urban. The urban population is expected to continue to grow, so that by 2050, the world will be one-third rural (34 percent) and two-thirds urban (66 percent). Figure 1.1 roughly the reverse of the global rural-urban population distribution of the mid-twentieth century (United Nations, 2014).

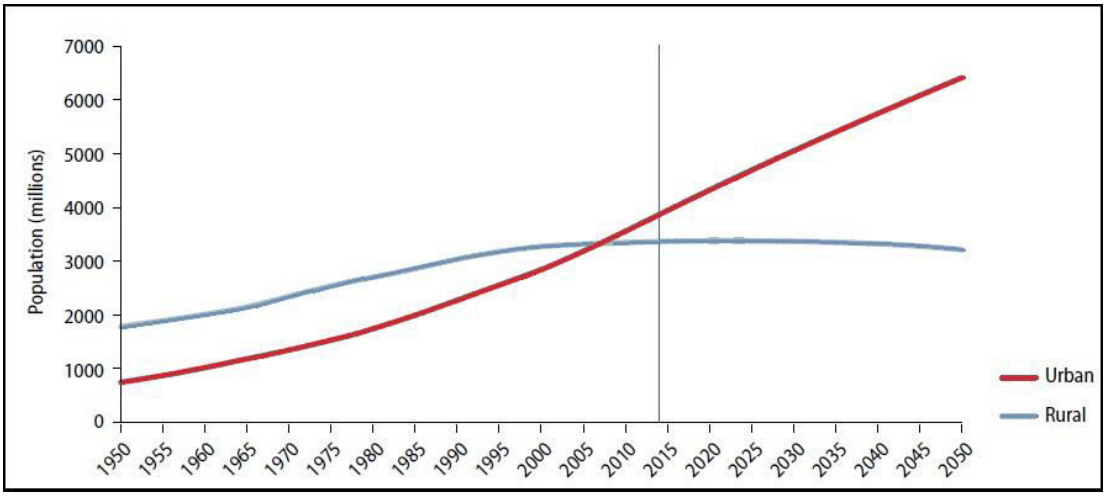

Figure 1.1.Urban and rural population of the world (1950–2050) (UN NGLS 2013).

Rapid urbanisation puts a considerable strain on housing and serviced land. Up to the year 2030, 3 billion people, or about 40 percent of the world's population need decent housing and access of to basic infrastructure and services such as water and sewage systems. These results will need to complete 96.150 units per day with the Earth service and documented from now until 2030. Every day, an increase of 120,000 people in addition to the population of Asian cities, require new housing at least 20,000 and support infrastructure. In Latin America and the Caribbean, the current housing needs are estimated between 42 million and 52 million homes, respectively. Estimates of the total housing needs in Africa are set at about 4 million units annually, with over 60 per cent of the demand necessary to accommodate urban inhabitants (UN-HABITAT 2014).

1.3. Relationship between LU/LC Changes and Land Surface Temperature

Understanding the relationship between land-use/land-cover change (LULCC) and the environment is seriously important to manage arid land. The conversion of land associated with agriculture and vegetation to those associated with population growth, urbanization and industrialization give rise to a considerable environmental problem. These problems include changes in the air temperature, changes in precipitation, and changes in the sunshine hours and land degradation.

Land use is converting over time, and the most important driving force of land use changes is the human need. Changing from permeable and moist land uses to impermeable and dry one with paving and building material can sharply affect energy budget and the temperature of land surface. As well as many other surface properties like the amount of evaporation, surface infiltration, runoff rate, drainage system (Guo, 2012).Cited by (Youneszadeh, 2013). Land surface temperature is gradually rising in all cities in the world due to increasing levels of land use change and conversion, especially in urban centers (Ogidiolu *et al.* 2013).

Weng (2001) say that, evident from recent studies that most cities around the globe have witnessed an increase in urban temperatures as urbanization of cities increases. The results of the urban expansion are increases in the number of buildings, extensive road networks, and other paved surfaces. Urban areas generally have higher solar radiation absorption, greater thermal capacity and heat is stored during the day and released by night. Built-up or urban areas tend to have relatively higher temperatures compared to those of non-urban areas. This thermal difference, combined with heat generated through urban houses, burning of fossil fuel in automobiles, and industry contribute to the development of "urban heat islands" (UHI) (Stemn, 2013).

Land cover and land use (LCLU) human-induced changes and natural processes play an important role in the global as well as in regional scale climate patterns and biogeochemistry of the Earth System. Geospatial technologies such as remote sensing (RS) and geographic information systems (GIS) are very effective at measuring and monitoring and prediction of land use/cover changes. Well timed information with the greatest possible accuracy of land use (LU) and cover (LC) changes of Earth is vital for long-term planning, economic development and sustainable management of natural resources.

The analysis of temporal remote sensing data helps in understanding the land cover changes and their impact on the environment. The thermal infrared bands of remote sensing data of spaceborne sensors help to retrieve land surface temperature (LST). LST is the measure of heat emission from land surface due to various activities associated with the land surface. Increase in paved land cover is an indication of concentrated human activities, which often leads to increased LSTs. Increased LST in certain urban pockets in comparison to its surroundings consequent to the increase in paved surfaces, is known as urban heat island (UHI) phenomenon (Ramachandra , 2012).

1.4. Remote Sensing for Analyzing Urban Expansion and Land Surface Temperature

Remote sensing can be defined as the art and science involving the detection, identification, classification, delineation, and analysis of earth surface features and phenomena using imagery acquired from terrestrial, aircraft and satellite platforms equipped with photographic and non-photographic sensors using visual and computer assisted interpretation techniques *(*Angel *et al.* 2005*)*.

Most researchers prefer thermal satellite data, because it has several significant advantages. For example, satellite data allow for the acquisition of data over large areas, while direct measurements provide point measurements. Another important advantage of RS data is its low price and the general simplicity of acquiring data, while to cover the whole region of interest with direct measurements will take lots of time and will be extremely expensive. It is also essential that the data from the sensor cover the region at one time with the same conditions *(*Bobrinskaya, 2012*)*.

Remote sensing of dwellings is increasingly used to provide detailed, up-to-date information. However, these remotely sensed datasets are mostly limited to local studies. Although high resolution and even very high resolution imagery with an almost global coverage are available, no consistent global coverage of settlements derived from those datasets exists. There are some global datasets derived from remote sensing that are applicable to urban studies, but they do not provide the necessary detail for many applications. To alleviate this lack of information, the Joint Research Centre (JRC) of the European Commission has recently developed an automated image information query system to produce a Global Human Settlement Layer (GHSL) from high-resolution optical imagery. This system is able to ingest high and very high spatial resolution imagery from

heterogeneous sources even with low quality (e.g. Lacking metadata, radiometric and geometric distortions). *(*GEO/Copernicus 2013*).*

Satellite imagery and GIS maps of land cover, land use and its changes is a key to many diverse applications such as environment, forestry, hydrology, agriculture and geology. Natural Resource Management, Planning and Monitoring programs depend on accurate information about the land cover in a region. Methods for monitoring vegetation change range from intensive field sampling with plot inventories to extensive analysis of remotely sensed data which has proven to be more cost effective for large regions, small site assessment and analysis. Evaluation of the static attributes of land cover (types, amount, and arrangement) and the dynamic attributes (types and rates of change) on satellite image data may allow the types of change to be regionalized and the approximate sources of change to be identified or inferred *(*Satellite imagine corporation*).*

1.5. Research Objectives:

1.5.1. General Objective

The aim of this study is to investigate the effects of urban expansion and land use/cover changes on land surface temperature (LST) in the city of Adana-Turkey and the urrounding areas between 1990 and 2011.

1.5.2. Specific Objectives:

- To determine LU/LC changes in the city Adana-Turkey between 1991 and 2011.
- To analyze the relationship between LST and NDVI.
- To evaluate the effects of urban expansion and LU/LC change on land surface temperature.
- To compare land surface temperature for different LU/LC types in the study area.

2. LITERATURE REVIEW

Tayanc and Toros (1997) evaluate urbanization effects on regional climate change in four urban stations in one developing country, Turkey, for the 1951–1990 time periods. The results revealed that the neighboring rural is a shift towards the warmer side in the frequency distributions of daily minimum and 21.00 hr temperature difference series. This shift is an indication of urban heat island. Also urban warming is detected to be more or less equally distributed over the year with a slight increase in the autumn months.

Weng (2001) evaluated that the urban growth and its impact on surface temperature in Zhujiang Delta of South China. Also integrated the remote sensing and (GIS) to examine the impact of urban growth on surface temperatures. The results revealed a notable and uneven urban growth in the study area. This urban development had raised the surface radiant temperature by 13.01K in the urbanized area.

As well as, Luck and Wu (2002) evaluates quantify the spatial pattern of urbanization in the Phoenix metropolitan area, Arizona, USA. They used landscape metrics with a gradient analysis approach. The results showed that the spatial pattern of urbanization could be reliably quantified, and the location of the urbanization center could be identified precisely and consistently with multiple indices.

However, Qin *et al.* (2002) analyses the seasonal and spatial change of land surface temperature (LST) in the Israel–Egypt border, to verify it through ground truth measurements and to simulate the average LST change on both sides according to surface composition structure. The results showed that in hot, dry summer the Israeli side is usually about 2.5–3.5°C hotter. In wet, cool winter the LST difference between the sides is not large, but the Israeli side still has higher LST. The Egyptian side may have slightly higher LST when surface temperature is below 20°C, several days after heavy rain, which leads to very wet surface conditions.

Gedik (2003) tested the differential urbanization theory in the Turkish case during the 45 years between1955-2000. The theory is first tested in the country as a whole, and subsequently for each of the three major regions with differing developmental levels. The findings for Turkey showed, in general, are consistent with the theory of differential urbanization. All regions are found to be in the early medium city. An interesting finding was that in the initial stages of urbanization experienced the growth of the small size cities instead of large cities.

Moreover, Sobrino *et al.* (2004) evaluates three methods to retrieve the land surface temperature (LST) from thermal infrared data supplied by band 6 of the Thematic Mapper (TM). They were present a comparison between the LST measured in situ and the retrieved by the algorithms over an agricultural region of Spain (La Plana de Requena-Utiel). The results showed a root mean square deviation (RMSD) of 0.009 for emissivity and lower than 1 K for land surface temperature.

On the other hand, Weng *et al.* (2004) estimates the relationship between land surface temperatures (LST) with vegetation, to analyses urban heat islands (UHI) of The City of Indianapolis. They used a Remote sensing technique according to the Normalized Difference Vegetation Index (NDVI) method. The results demonstrated that (LST) possessed a slightly stronger negative correlation with the unmixed vegetation fraction than with NDVI for all land cover types.

Van (2005) evaluated the relationships between urban surface temperature and land cover types and the solution to the reduction of heat island effect In the Hochiminh City Commercial center in Vietnam. The Results showed thermal energy responses of different land forms in study area indicate the variation in surface temperature of different surface patterns. The Analysis from imagery indicated that the industrial, residential areas are places with highest surface temperature relative to vegetation and water exhibiting lower temperature

Angel *et al.* (2005) evaluates the dynamics of global urban expansion by defining a new universe of 3,943 cities with a population in excess of 100,000 and drawing a stratified global sample of 120 cities from this universe. The results showed that If average densities continue to decline at the annual rate of 1.7% as they have during the past decade the built-up area of developing-country cities will increase from 200,000 km2 in 2000 to more than 600,000 km2 by 2030, while their population double.

Likewise, Oguz (2005) evaluated simulate future on urban growth in the Houston metropolitan area, one of the fastest growing metropolises in the United States during the past decades, for the period from 2002 to 2030. He used SLEUTH, a spatially explicit cellular automata model; the result showed that the spatial pattern of urban growth of the Houston CMSA is predicted predominantly “organic” with most growth occurring along the urban/rural fringe.

Yuan and Bauer (2007) analyses, comparison between the normalized difference vegetation index (NDVI) and percent impervious surface as indicators of surface urban heat island effects in Landsat imagery by investigating the relationships between the land surface temperature (LST), percent impervious surface area (%ISA), and the NDVI. Landsat Thematic Mapper (TM) and Enhanced Thematic Mapper Plus (ETM+) data were used to estimate the LST from four different seasons for the Twin Cities, Minnesota, metropolitan area. This analysis indicated there is a strong linear relationship between LST and percent impervious surface for all seasons, whereas the relationship between LST and NDVI is much less strong and varies by season.

Reis (2008) investigated LULC changes by using of Remote Sensing and Geographic Information Systems (GIS) in Rize, North-East Turkey. The results indicated that severe land cover changes have occurred in agricultural 36.2% (Especially in tea gardens), urban 117%, pasture -72.8% and forestry -12.8% areas has been experienced in the region between 1976 and 2000. It was seen that the LULC changes were mostly occurred in coastal areas and in areas having low slope values.

In addition, Van *et al.* (2009) evaluates the surface temperature of urban areas in Ho Chi Minh City considered surface emissivity factor from NDVI method. The experiment was carried out on Landsat and Aster satellite images that are suitable for studies on heat processes in urban areas. The results showed that the average bias of LST calculation is about 2oC in comparison with the in-situ measurements.

Mbithi *et al.* (2010) assesses the impact of Land Use Land Cover (LULC) changes on land surface temperature in the capital of Ethiopia, Addis Ababa from 1986 to 2010. The results showed that the observed changes in LULC were largely attributed to population pressure on the land, a rapidly growing infrastructure and poor land use planning. Changes in LULC were accompanied by changes in Land Surface Temperature (LST) leading to an intensified Urban Heat Island (UHI) effect in the urban areas. Moreover, the urban-rural temperature differences between the urban core and its surrounding areas showed a maximum difference of more than 20°C.

Saleh (2011) evaluated the impact of urban expansion on surface temperature in Baghdad, IRAQ. The results indicated that the distribution of urban surface temperature was very different depends on various land cover types of surrounding areas.

Ahmed *et al.* (2011) Investigate the spatial distribution property of land surface temperature (LST) and evaporate transpiration (ET) over the Gezira area. Images in visible, near infrared and thermal infrared regions of the electromagnetic spectrum were processed to extract surface radiant temperature, Normalized Difference Vegetation Index (NDVI), and land cover types. The results of the regression between extracted land surface temperature, NDVI and evaporate transpiration show negative (-) correlation. As well as, demonstrated that LST possessed a slightly stronger negative correlation with the (ET) than with (NDVI) for all land cover types.

Rahman *et al.* (2011) investigates urbanization and the Quality of the urban environment in East Delhi-India. They used Landsat ASTER (MSS) data on comparison quality of environment between 1982 and 2003. The result showed that the Most of the Eastern district was in a better state of the environment in 1982, but in 2003 things have been changed and now 50% area is in very good, fair and desirable condition.

Also, Azim and Islam (2011) prepared a model for estimating land surface temperature in New Delhi and its surroundings from Landsat Thermal Imagery. Emissivity was retrieved from satellite data by using the Normalized Difference Vegetation Index (NDVI) and used in modeling to ensure least error. The result of the research showed the structures of the model. It also showed the spatial variation of land surface temperature. Comparisons showed how precise estimated land surface temperature was in respect of any land observation data.

Ramachandra *et al.* (2012) investigates quantify the changes in the land cover and consequent changes in land surface temperature of India. The thermal infrared bands of the Landsat data were used to retrieve land surface temperature. The results revealed that there was a huge increase in urban area (including barren land), which is the causal factor in the changes in land surface temperature.

At the same time, Omran (2012) investigated the application of RS/GIS for detecting LU/LCC and its impact on surface temperature in the Ismailia Governorate, Egypt. Also utilized Landsat images to quantify the changes from 1984 to 2011. The results revealed a notable land-use change in the study area. The Built-up area has rapidly increased in Ismailia during the 27 year period.

Chima (2012) evaluated analyzing urban Land Use and Land Cover (LULC) by Object Based image Analysis (OBIA) method in Abuja-Nigeria. Used Nigeriasat-1 satellite data. The result showed that the drivers of land use and land cover change in Abuja are similar to those of planned capital cities in other developing economies. Also Land use developments in Abuja can provide an insight into urban dynamics in a developing country's capital region.

Bobrinskaya (2012) evaluated the relationship between land use and land cover types and corresponding land surface temperature over a 10 years period in the 10 mega cities around the world. The results indicated that land surface temperature can be related to land use/land cover classes in most cases. Also vegetated and undisturbed natural areas enjoy lower surface temperature than developed urban areas with little vegetation.

Also, mega cities of developed countries tend to grow at a slower pace and thus face less urban heat island effects than mega cities in developing countries.

Wang (2012) analyzed urban sprawl and sustainable development in China By using the program SPSS for 15 top urban regions in China during 10 years. The result showed that the causes of urban sprawl in China are raising private automobile ownership, rising demand for space and changing residential preference, local public policy, and the real-estate industry.

At the same time, Jibril *et al.* (2012) evaluates the impact of urban growth on land surface temperature in FCT, Abuja. They used remote sensing and GIS techniques to identify the various land uses, their various transformations between 1986 and 2006 and measures the rate of urban expansion and loss of vegetation cover. The results revealed that the built up area has expanded by 17.88% of the total land area of Abuja in 1986 to 27.02% in 2006, vegetation covers reduced from 47.23% to 37.79%.

Ogidiolu *et a.,l* (2013) examines the pattern of surface temperature change between (1987, 2001, and 2011) In the Federal Capital Territory of Nigeria. The result revealed a rapid growth in built-up land between 1987 and 2001 while the periods between 2001 and 2011 also witnessed a massive increase. The was also projected that by 2025 built up land would have taken over 50% of the entire land mass of Federal Capital Territory FCT, which may also go along with the increase in surface temperature with its consequence for human.

On the other hand, Buyadi *et al.* (2013) investigates the effects of land use changes on the surface temperature of the National Botanic Garden, SHAHALAM and the surrounding areas, of 1991 and 2001. They were using remote sensing and geographical information system (GIS) techniques. The Results obtained have shown that the LST of different land use differs significantly. This study demonstrates that rapid urban growth significantly decreases the vegetated areas, hence increased the surface temperature and modified the urban microclimate.

It is also, Ahmed *et al.* (2013) evaluates the land cover dynamics and their impacts on land surface temperature (LST) of Dhaka Metropolitan (DMP). They used Landsat satellite images of 1989, 1999, and 2009 for analysis. Simulation results showed that if the current trend continues, 56% and 87% of the DMP area will likely to experience temperatures in the range of greater than or equal to 30 °C in 2019 and 2029, respectively.

Oguz (2013) evaluated a computer program, the Land Surface Temperature Calculator (LST Calculator). He used a Landsat Enhanced Thematic Mapper Plus (ETM+) image of Dallas – Fort Worth Metroplex as a case study for demonstration purposes. The results showed that The LST Calculator is a helpful and valuable tool to study thermal environments.

Akin *et al.* (2013) evaluates that, the integration of remote sensing and GIS techniques to characterizing the spatiotemporal trends of land use/land cover change in the city of Adana- turkey. They were analyses (LU/LC) change performed by considering the metric calculation. The result showed that the most considerable change was observed in the agricultural areas. Also Urban sprawl is the major driving factor of the (LU/LC) change.

Subsequently, Stemn (2013) assessed urban expansion effects on surface temperature in the Metropolis of the years 1991 and 2008. He used an integrated remote sensing and GIS approach. The results showed that there has been a significant urban growth in the study area with an annual rate of change of land cover of 4.06%. Also the annual rate increase in urban/built-up land was determined to be 4.65%. This urban development had increased surface radiant temperature in the study area by 4.3°C in the urbanized areas.

At the same time, Youneszadeh (2013) investigated the application of remote sensing, geographic information systems (GIS) and statistical methods to provide quantitative information on the effect of land use on land surface temperature. The results showed that the Night land surface temperature correlates positively with the coverage percentage of open agriculture, forest and greenhouse farming. Also showed inland water and offshore area has the highest night LST and the lowest day LST. The Build-up is the warmest land use during the days and the second warm land use during the night time.

Also, Balçik (2014) the effect upon the urban heat island (UHI) of Istanbul was analyzed. Used 2009 dated Landsat 5 Thematic Mapper (TM) Data. The results showed that artificial surfaces have a positive exponential relationship with LST rather than a simple linear one. Also an ecological evaluation index of the region was calculated to explore the impact of both the vegetated land and the artificial surfaces on the UHI. At the same time she suggested that the areas with a high rate of urbanization will accelerate the rise of LST and UHI in Istanbul.

3. MATERIALS AND METHODS

3.1. Materials

3.1.1. Study area

Adana is fifth of the largest cities in Turkey, with a history dating back to six thousand BC. It is a very advanced area of geographical, economical and cultural. The city has a fertile land, also is one of the most agriculturally productive areas of the turkey. Adana is the marketing and distribution center for Çukurova. The city has great quantities agricultural products, such as: cotton, citrus, corn, wheat, soybean, barley, grapes, orange, and fruits who that has a significant role in the economy of the city.

Adana has a typical Mediterranean climate, summers are hot and dry and winters are mild and wet. The average temperature is somewhat warm at 19 degrees Celsius. The hottest month is August with a mean temperature of 28 degrees Celsius. January is the coldest month with a mean temperature of 9.7 degrees Celsius (climate map 2013). Figure 3.1 is a monthly temperature graph of Adana-Turkey. Indeed, significant changes in land use have been observed in the city with surrounding areas. Space of the study area is 351562.59 hectares; urban areas with 9.78 % in 1990 and 16.96 % in 2011 in total area. Also, the city of Adana is growing rapidly in the period after 1950. According to Turkey Statistical Institute (TUIK), number of population in the Province of Adana as of December 31, 2014 is 2,125,635. Also, the population in the city Adana is 1,663,485.

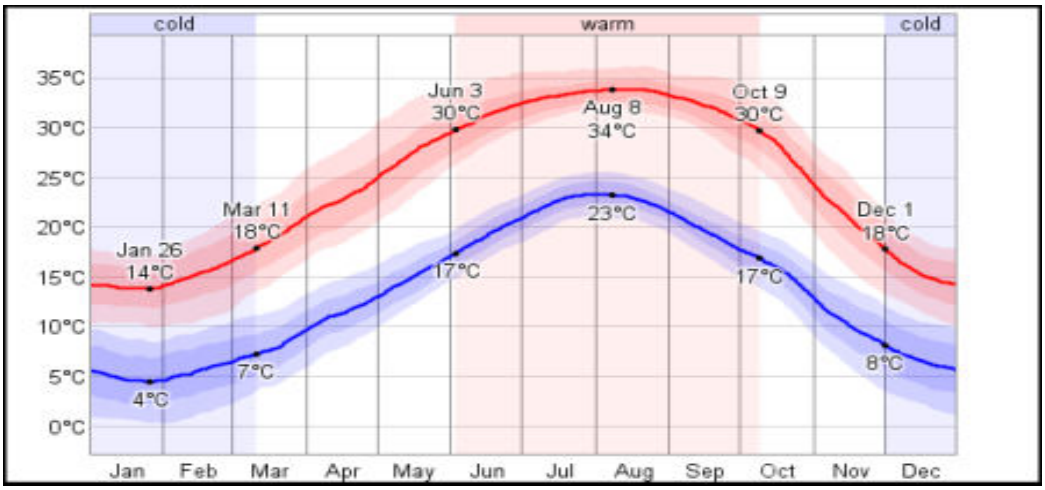

Figure 3.1 Showing monthly temperature of Adana, Source (climate map 2013)

By Geographical and astronomical location, Adana located 30 km inland from the Mediterranean over the Seyhan River. The city is located at the Southeastern Mediterranean coast of Turkey. It is situated on the river (Sayhan), and lies in the (Çukurova). Adana is the main gateway for transportation between Cyprus and Anatolia. On the other hand, the city is the major transportation routes connecting Europe to Asia. The latitude is 36°00'- 37°30' and longitude is 34°30'- 36°00'. Altitude in the Adana ranges from sea level to 3679 m, with a mean altitude of 1271 m above sea level (Berberoglu *et al*., 2007). Figure 3.2 is a map of the study area.

Figure 3.2. Map of Turkey Showing the Study Area

3.1.2. Data

The study was based on the use of a time series of satellite Landsat images - Thematic Mapper (TM). The primary sensor aboard Landsats 1, 2, and 3 was the multispectral scanner (MSS). The resolution of the MSS sensor was approximately 80 m, with radiometric coverage in four spectral bands from the visible green in the near-infrared (IR) wavelengths. Landsats 4 and 5 carried both the MSS and a new, improved thematic mapper (TM) sensor. TM bands 1-5 and 7 collect reflected energy; band 6 collects emitted energy. The TM sensor has a spatial resolution of 120 m for the thermal- IR band and 30 m for the six reflective bands.

The newest satellite in the series, Landsat 8, carries the enhanced thematic mapper plus (ETM+), with 30-m visible and IR bands, a 60-m spatial resolution thermal band, and a 15-m panchromatic band (USGS, 2003). These sensors support the Landsat Project's mission to provide quality remote sensing data in support of research and applications activities.

In this study used landsat 5 TM data for the years 1990 and 2011, were downloaded from the official website of US Geological Survey (USGS). The data acquisition date has a highly clear atmospheric condition. The Landsat 5 TM sensor acquires data in seven spectral bands with the pixel sizes of the images 30 × 30 m. Table 3-1 shows the data types that were used during the study. Bands 1-5 &7 were used for LU/LC classification, also band 6 for LST extraction. Figure 3.3 shows the Landsat images that were used for the study.

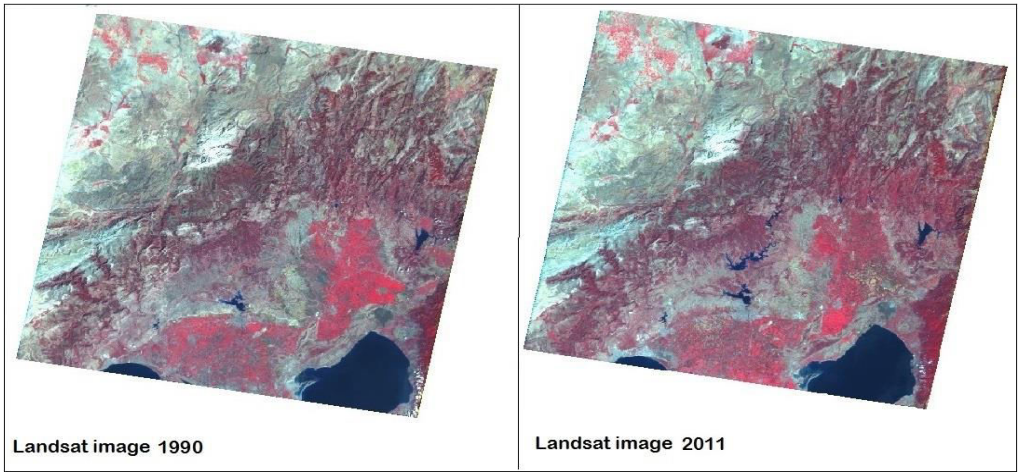

Figure 3.3. Landsat 5 TM Imagery used for the Study. Source (USGS)

Table 3.1. Data types used for the Study

Satellite images	Landsat 5	Landsat 5
Acquisition Date	29, Aug 1990	23, Aug 2011
Sensor	TM	TM
Resolution	30 X 30	30X30
Data Source	USGS	USGS
Format	Geo Tiff	Geo Tiff
No: Bands	7	7

3.1.3. Software

In this research used ERDAS Imagine 9.2 for the image processing, including pre-processing, image classification, accuracy assessment, production of a change map and image transformation. ERDAS imagines perform advanced remote sensing analysis and spatial modeling to create new information. In addition, with ERDAS imagine, you can visualize your results in 2D, 3D, movies, and on cartographic-quality map compositions. The core of the ERDAS imagines product suite is engineered to scale with your geospatial data production needs. Optional modules (add-ons) providing specialized functionalities are also available to enhance your productivity and capabilities (Intergraph, 2013).

As well as, Arc GIS 10.2.1 was used to generate the output maps and also used to carry out all the GIS analysis that was done. Geographic Information System (GIS) is an organized collection of computer hardware, software, geographic data and personnel designed to efficiently capture, store, update, manipulate, analyses, and display all forms of geographically referenced information. GIS Is software represents features of the earth, such as buildings, cities, roads, rivers, and states, on a computer. Often, this data is viewed on a map, which provides an advantage over using spreadsheets or databases. GIS benefits organizations of all sizes and in almost every industry. There is a growing interest in and awareness of the economic and strategic value of GIS (ESRI, 2007).

On the other hand, the (LST) Calculator software was used to calculation land surface temperature. This software is helpful to Retrieving land surface temperature from landsat TM/ETM+ Imagery easily who created by (Oguz 2013).

At the same time, I used Microsoft Office excel to calculate LST, also to finding Relationship between NDVI and LST. Likewise, used Google map and being map during the classification image for determination land cover components correctly.

3.2. Methods

A technological approach was used to develop a method to characterize land use change from the analysis of GIS and remote sensing data. This approach is utilized to shows urban expansion and effects on land surface temperature in the city of Adana with surrounding areas. The methodology in this research is divided into three main categories: (1) data processing, (2) LST retrieval and (3) relationship between NDVI and LST. These parts have sub-part. All of them are described in the figure 3.4. The two satellite images were selected to differentiate the land use changes from two dates separately over a period of 21 years. Urban expansion detection and analysis Land use/cover patterns for 1990 and 2011 were mapped by the use of Landsat Thematic Mapper (TM) data.

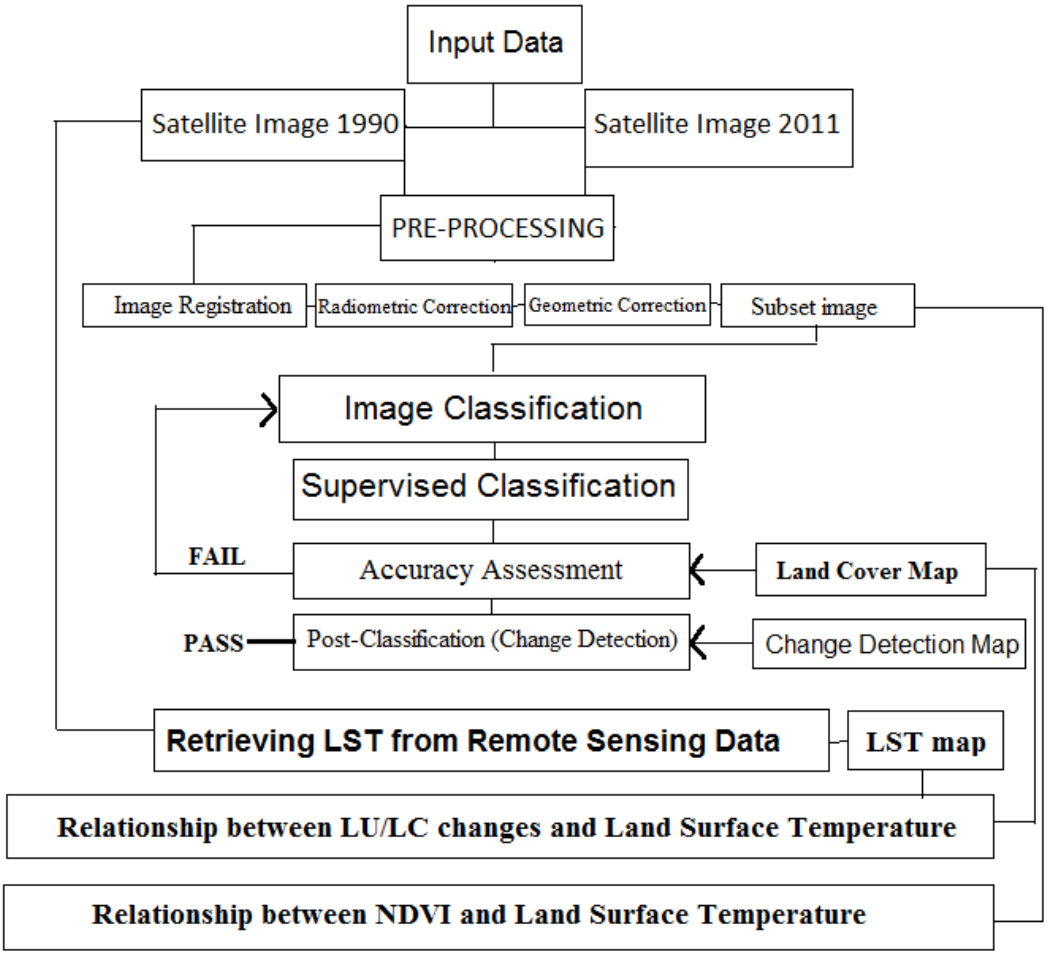

Figure 3.4. Flowcharts summarizing the methodology

3.2.1. Pre-processing

Data pre-processing is an extremely important stage of satellite imagery processing and analysis, which has an impact on all further actions and final product quality. Pre-processing usually consists of a sequence of operations, Main steps include: radiometric correction, geometric correction and image registration. Accurate and precise registration of multi-temporal image is extreme important in change detection studies. These steps are usually required before remotely sensed data are analyzed. This is because a mis-registered image will lead to the production of wrong change detection and vice versa. Therefore, the integrity of change detection depends on the accuracy of the image rectification.

3.2.1.1. Image registration

Image registration can only be done when the individual bands of satellite images are combined into a single image (Stemn 2013). Landsat imagery comes in (GeoTIFF) image format with each spectral band in a separate file. Before further processing, bands were stacked in one image file, excluding unnecessary bands. Thus with the aid of the Layer Stack tool in the Utility toolbar of ERDAS Imagine 9.2, of all the two images 1990 and 2011 were combined in to a single image.

3.2.1.2. Radiometric correction

One common cause of radiometric error is sensor malfunction. Radiometric resolution refers to the dynamic range, or number of possible data files values in each band. Radiometric correction is used to normalize data taken at different time and location (i.e. at different conditions), so that the spectral values of the same pixels would be the same. Two types of sensor malfunction are line start error and bad lines. Usually bad lines appear white color. In this particular study no radiometric correction was done, because the datasets obtained were already corrected to some extent by the USGS.

3.2.1.3. Geometric correction

Geometric correction serves to eliminate geometric distortions of the raw data due to the different factors, for example (motion of the sensor, perspective of the optical scheme, terrain and other). Generally, geometric correction re-projects the image from the sensor's projection to the proper projection and coordinate system. The original satellite images obtained were in Global Coordinate System, UTM WGS 84. The Geo-reference

image produced a root mean square value of 0.5 the rectified 1990 and 2011 TM image was used to Geo-reference.

3.2.1.4. Subset image

By using the subset tool in the Data Preparation toolbar of ERDAS Imagine, subsets were generated for the two images in order to extract the study area for consideration. Generally, four ways we can use to subset image in ERDAS Imagine; that is (AOI) tool (drawing manually), subset image by specific Coordinates, by inquire box, and subset image by shape file. The shape file was used in creating the subsets. After registering the images, a subset area of image was extracted. Figure 3.5. shows the subset images that were generated.

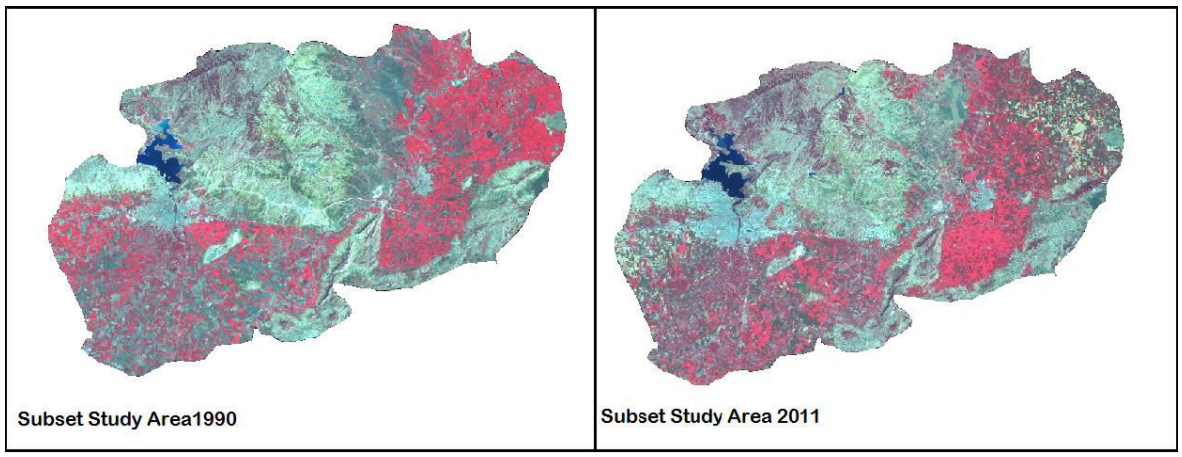

Figure 3.5. Subset image showing only the study area

3.2.2. Image classification

Land cover classification is the classification of satellite images based on the reflected signals from the earth surface materials. Land use classification considers the socio-economic activity of the location of interest and is interpreted from the land cover in the context of surrounding features (Chima, 2012). The objective of image classification is to assign a land cover/land use class or any other thematic class to each pixel of the image, based on its spectral characteristics. There are two types for image Classification: supervised classification and unsupervised classification. Supervised classification is user will be classifying components, but unsupervised classification is an automatic classification type. In this research used supervised classification.

3.2.2.1. Supervised classification

Supervised classification was used to classify the individual images into the various land cover classes. Training samples of all the various land cover types. The six land use/land cover types identified from these two Landsat images are; Urban, Forest, Agriculture, Water, Grassland, and Other on the 1990 and 2011image. Table 3.2 is a description of the various land cover classes. These six training sites which represented the six cover types used in this study were named and saved in the Signature Editor in the Classifier Tool of ERDAS imagine. As well as (Google Earth and Being map) was used for determination land cover types correctly of each training area for a specific class. This process was effectuated for the two images separately.

After the generation of signatures, the next stage of the classification process was the classification stage itself. Using the Supervised Classification tool in ERDAS imagine as well the signatures that were saved, the 1990 and the 2011. The land use/land cover maps of these two dates are generated from these two images in the ERDAS Imagine digital image processing software.

Table 3.2. Description of the Land Cover Classification System Used in the Study

Cover Class	Description
Urban	The categories in this area are residential area (cities, towns and villages), highways and transportation, communications facilities, commercial area, and administrative building.
Forest	Forest Lands have a tree areal density, stocked with trees capable of producing timber or other wood products, and exert an influence on the climate regime. Also forest lands include deciduous, evergreen and mixed forest lands, parks and bushes.
Agricultural	Agricultural land may be defined broadly as land used primarily for production of food and fiber. This category includes: cropland and pasture, horticultural areas.
Grassland	Grasslands are areas where the vegetation is dominated grasses occur naturally. They contain many grass species and an even greater diversity of other herbs.
Water	This category includes: streams and canals, lakes, reservoirs, bays and estuaries.
Other	It is a land of limited ability to support life and in which less than %5 of the area has vegetation or other cover. Includes: fallow land, sand land, open space, bare land.

3.2.3. Accuracy assessment

Image classification is not valid without assessment of its accuracy. After completion of the classification exercise it was necessary to assess the accuracy of the results obtained. One of the most common methods of classification accuracy assessment is error matrix or confusion matrix. This matrix contains a category comparison of relationship between known, ground-truth data and classification results for the same category (Bobrinskaya, 2012). The accuracy of the land cover maps generated from the individual images was assessed. The accuracy of the classification was verified by field checking or comparing with existing land use and land cover maps that have been field-checked. Using the Accuracy Assessment tool in ERDAS imagine, also selected 180 random points for two images 1990 and 2011.

3.2.4. Change detection

A classified image often has some misclassified pixels. In this study I used Change detection to highlight or identify significant differences in imagery acquired at different times. ERDAS imagine provide two tools for change detection: (1) under the Image Interpreter button From Utilities, the Change Detection operation allows for two continuous images as input. (2) The Matrix operation from the GIS Analysis menu allows for two thematic images or vector files of different years to be compared.

The matrix contains a category comparison of relationship between known, ground-truth data and classification results for the same category. The overall accuracy shows the overall accuracy of the classification process. Hence, The Matrix Module in ERDAS Imagine was used to investigate the land cover changes that have occurred in the study area. The transition contingency matrix was also generated to test the independence or association that existed between the land cover classes in the different years. A matrix was generated from the thematic maps (classified image) 1990 – 2011. The elements in the off-diagonal of the contingency matrix represent land cover classes that have changed whiles the elements in the diagonal shows unchanged land cover classes.

3.2.5. Retrieving LST from remote sensing data

Land surface temperature (LST) is an extremely important parameter that controls the exchange of long wave radiation between the surface and atmosphere. Because of the

extreme heterogeneity of most natural land surfaces, LST is a difficult parameter to estimate and to validate (Prata, 2000).

On the other hand, (Yang, 2012) say that the Land surface temperature (LST) is generally defined as the skin temperature of the ground. LST in remote sensing can be defined as the average surface temperature of the ground under the pixel scale mixed with different fractions of surface types. One of the most widely used to retrieve land surface temperature nowadays is to employ thermal infrared remote sensing data (bobrinskaya, 2012). There are various algorithms to estimation LST, such as: viz, Split-Window (SW), Dual-Angle (DA), Single-Channel (SC), Sobrino and Mao, Temperature and Emissivity Separation (TES), (Rajeshwari & Mani, 2014).

There are three different single-channel methods: i) the Radiative Transfer Equation (RTE), ii) Qin et al.'s (2001) algorithm, and iii) Jimenez- Munoz and Sobrino's (2003) algorithm, (Oguz, 2013). In this research, the RTE of single - channel methods were used for Landsat 5 ™ sensor) data. The LST of 1990 and 2011 is obtained by applying the following equations. Figure 3.6 as shown the methodology.

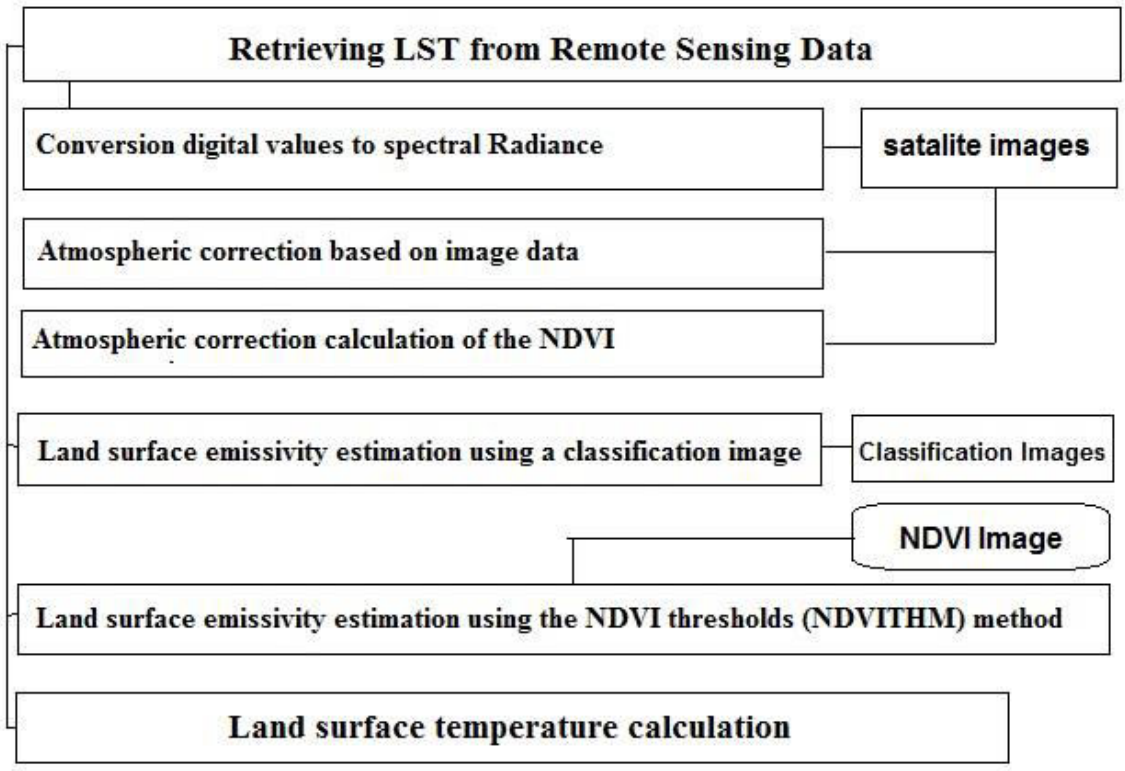

Figure 3.6. Show the methodology of Retrieval LST.

3.2.5.1. Conversion digital values to spectral radiance

The Landsat Thematic Mapper (TM) and Enhanced Thematic Mapper Plus (ETM+) sensors acquire temperature data and store this information as a digital number (DN) with a range between 0 and 255. It is possible to convert these DNs to TOA Reflectance (The Yale Center for Earth Observation 2013). However, used Spectral Radiance Scaling Method to convert (DN) to spectral radiance values according to equation 1. The data is saved as Land surface emissivity measured in Kelvin.

$$L_\lambda = \frac{L_{max} - L_{min}}{QCAL_{max} - QCAL_{min}} \ (DN - QCAL_{min}) + L_{min} \quad \text{(Eq.1)}$$

Where: Lλ = spectral radiance at the sensor's aperture in W/(m2 sr μm); QCALmax = the highest point of the rescaled radiance in DN; QCALmax = the lowest point of the rescaled radiance in DN (1 for LPGS, 0 for NLAPS); Lmax = the TOA radiance that is scaled to QCALmax in W/(m2 sr μm); Lmin = the TOA radiance that is scaled to QCALmin in W/(m2 sr μm).

3.2.5.2. Atmospheric correction based on image data

This method was developed by Chavez (1996), and its main advantage is that the data necessary in order to carry out the atmospheric correction are obtained from the image itself (Sobrino et al., 2004). For this purpose, the at-surface reflectivity is calculated with the equation 2.

$$\rho_P = \frac{\pi.(L_\lambda - L_h).d^2}{ESUN_\lambda.cos\theta_s.\tau} \quad \text{(Eq.2)}$$

Where: ρP = atmospherically corrected unitless planetary reflectance; Lλ = spectral radiance at the sensor's aperture; Lh = radiance resulted from the interaction of the electromagnetic radiance with the atmospheric components (molecules and aerosols); d = earth-sun distance in astronomical units; ESUNλ = mean solar exoatmospheric irradiances; θs = solar zenith angles in degrees; τ = the atmospheric transmissivity.

L_h can be obtained according to Equation 3.

$$L_h = L_m - L_{1\%} \quad \text{(Eq.3)}$$

Where: Lm = the radiance that corresponds to the dark object DN value; L1% = 1 percent of the theoretical radiance of a dark object.

L_m can be computed in Equation 4.

$$L_m = L_{min} + DN_{min}\left(\frac{L_{max} - L_{min}}{QCAL_{max}}\right) \quad \text{(Eq.4)}$$

Where: DN_{min} = the dark object DN value (minimum DN value).

The term $L_{1\%}$ is given by Equation 5.

$$L_{1\%} = \frac{0.01.\cos\theta_s.\ \tau.\ ESUN_\lambda}{\pi.d^2} \quad \text{(Eq.5)}$$

τ can be obtained according to Chavez (1996) in Equation 6.

$$\tau = \cos\theta_s \quad \text{(Eq.6)}$$

3.2.5.3. Atmospheric correction calculation of the NDVI

Many images are contaminated with haze, clouds, and cloud shadows, which greatly limit their effective utilization. Many efforts have been made to retrieve surface reflectance from Landsat TM imagery by correcting atmospheric effects (Liang *et al.,* 2002).

On the other hand, (Hadjimitsis *et al*., 2010) reckon that, the Radiation from the Earth's surface undergoes significant interaction with the atmosphere before it reaches the satellite sensor. This interaction with the atmosphere is stronger when the target surfaces consist of non-bright objects, such as water bodies or vegetation. This problem is especially significant when using multi-spectral satellite data for monitoring purposes, such as agricultural or land use studies. He believed that the Normalized Difference Vegetation Index (NDVI) is the most common and known vegetation index and has been proposed by (Rouse *et al*., 1974).

However, the sensitivity of the NDVI on atmospheric effects has generated an increasing interest in the development of new vegetation indices which are less sensitive to atmospheric effects. Moreover, (Sobrino *et al.,* 2004) mentions that, (Vermote *et al.,* 2002) also reported that the NDVI values, on average, increased from -0.26 to 0.10 after atmospheric corrections. The data supplied by bands 3 and 4, located in the red and near infrared, respectively, can be used to construct this vegetation index according to the equation 7.

$$NDVI = \frac{\rho_{band4} - \rho_{band3}}{\rho_{band4} + \rho_{band3}} \quad \text{(Eq.7)}$$

Where: ρ_{band4} = the spectral reflectance of near infrared band (band 4); ρ_{band3} = the spectral reflectance of red band (band 3).

3.2.5.4. Land surface emissivity estimation using classification images

Before using this method, the user is required to classify the satellite image (Landsat TM/ETM+) into classes of land use/land cover using one of the image processing packages such as Erdas Imagine, ENVI etc. the classified image and the emissivity values are very critical in this method. The final LST result depends solely on the classification accuracy of the classified image and the emissivity values for the land cover classes (Oguz, 2013).

Though, (sobrino *et al.,* 2004) reckon that, the possible alternative could be to obtain an LSE image from a classification image, in which an emissivity value for each class is assumed. However, this is not very operative because we need a good knowledge of the study area and emissivity measurements on the surfaces representatives of the different classes and coincident with the satellite overpasses (i.e., the vegetative cover of the agricultural areas could change with time).

3.2.5.5. LSE estimation using the NDVI thresholds (NDVITHM) method

Emissivity is an important factor that affects the observed surface temperature change by detecting the thermal radiation (Qin *et al.,* 2002). Also (Van *et al*., 2009) says that, the pixels representing the land surface are usually mixed pixels of surface types such as vegetation and soil. To estimation land surface emissivity NDVI thresholds (NDVITHM) method was used during the atmospheric correction process.

This methodology originally introduced by (Sobrino and Raissouni 2000) and modified later by (Stathopoulou *et al*., 2007). On the other hand, (Vahmani and Hogue 2014) and (Sobrin*, et al.,* 2001) considers three different types of pixels depending on the NDVI value:

(a) NDVI < 0.2 In this case, the pixel is considered as bare soil and the emissivity is obtained from reflectivity values in the red region.
(b) NDVI>0.5 Pixels with NDVI values higher than 0.5 are considered as fully vegetated, and then a constant value for the emissivity is assumed.
(c) ($0.2 \leq NDVI \leq 0.5$) In this case, the pixel is composed of a mixture of bare soil and vegetation (sobrino *et al.,* 2004) and (Sobrino *et al*., 2002). The emissivity is calculated according to equation 8.

$$P_v = \left(\frac{NDVI - NDVI_{min}}{NDVI_{max} - NDVI_{min}} \right)^2 \quad \text{(Eq.8)}$$

where: $NDVImax = 0.5$; $NDVImin = 0.2$

3.2.5.6. Land surface temperature calculation

The atmospheric parameters can be calculated by using a Radiative Transfer Code like MODTRAN. MODTRAN1"2 is a new atmospheric radiance-transmittance code based on LOWTRAN with increased spectral resolution (Acharya *et al*., 1993).

In this study, an atmospheric correction tool, which uses the MODTRAN (RTC) developed by (Barsi *et al*., 2005) for the thermal band of Landsat TM was applied. This tool estimates three parameters - atmospheric transmission, upwelling radiance, and down-welling radiance. Once these parameters are retrieved, it is possible to convert the space-reaching radiance or TOA radiance to surface leaving radiance (Oguz, 2013). Calculated land surface temperature by using equation 9.

$$L_T = \frac{L_\lambda - L_\mu - \tau(1-\varepsilon)L_d}{\tau . \varepsilon} \quad \text{(Eq.9)}$$

Where: LT = radiance of a blackbody target of kinetic temperature T; Lλ = the space-reaching or top of atmospheric radiance; Lμ = the upwelling or atmospheric path radiance; Ld = the down welling or sky radiance; τ = the atmospheric transmission; ε = the emissivity of the surface.

The radiances are in units of W/(m2 sr μm), while the transmission and emissivity are unitless. The land surface temperature was calculated using the equation 10, (Chander and Markham, 2003).

$$T = \left(\frac{K_2}{In\left(\frac{K_1}{L_T} + 1 \right)} \right) - 273.15 \qquad \text{(Eq.10)}$$

where: T = the temperature in Kelvin (K); $K1$ = the pre-launch calibration constant 1 in W/(m2 sr μm); $K2$ = the pre-launch calibration constant 2 in Kelvin; LT = the radiance of a blackbody target of kinetic temperature T in W/(m2 sr μm).

3.2.6. Relationship between LU/LC and Land Surface Temperature

To determine the relationship between LU/LC changes with land surface temperature reclassified both images 1990 and 2011 that were classified before to separation type of class separation. After that, imported into (ArcGIS) also converted to Grid format. Afterwards, the specific LU/LC map was masked with the corresponding LST by using the extract by mask function in ArcGIS by all 12 LU/LC shape files separately. For example, LST was masked with the urban shape file of the year 1990 and named (Urban-mask 90). This approach was repeated for the other 11 LU/LC shape files for the different years. For each LULC class minimum, maximum, mean land surface temperature has been calculated. After that, an excel sheet was created for each land use class, including the percentage of each year. Thus, we can show on how the classes and corresponding LST have changed from 1990 to 2011.

3.2.7. Relationship between NDVI and Land Surface Temperature

To determine the relationship between NDVI and LST, the LST and NDVI images of the study area are analyzed with the aid of ERDAS imagine and GIS the software. First of all, NDVI map has been extracted from original Landsat imagery for the years 1990 and 2011. NDVI can be calculated from visible and near infrared bands, as NDVI value is related to LU/LC class. After that, from Accuracy assessment in ERDAS imagine collected 40 random points to NDVI image 1990, and then selected all points to preview on the image. Afterwards, viewed corresponding LST image on the separate viewer also linked those points by right click on the NDVI image and click on Gio.link.

After that, linear regression between NDVI and LST has been calculated manually. For this process, created excel sheet and wrote each value from LST and NDVI maps one by one according to X.Y points. Finally, I found (R^2) and correlation. This approach was repeated for the NDVI and LST images in 2011.

4. RESULTS AND DISSCUSION

4.1. Image Classification

In the beginning of work, the individual bands of each satellite images 1990 and 2011TM are stacked into a single image, also geometrically corrected to a classification process. The maximum likelihood algorithm (MLA) to each image has been applied according to the covariance and variance of the spectral response patterns of a pixel. This method is similar with some other researches. Such as: (stemn, 2013), (Ramachandra *et al*., 2012).

Thus, Figure 4.1 a graphical representation of the extent of area of the individual land cover types depicting of the six land cover changes in 1990 and 2011, also the percentages they occupy. As well as, the two land cover maps that were obtained as shown in Figure 4.2 and 4.3. In addition Table 4-1 shows the area extent of the individual land cover categories in hectares (ha). The table shows that, in 1990 (Agricultural) land were the dominant land cover type in the study area, covering an area of 192223.89 ha, 54.67%. However, in 2011 decreased to 190451.97 ha, 54.17%.

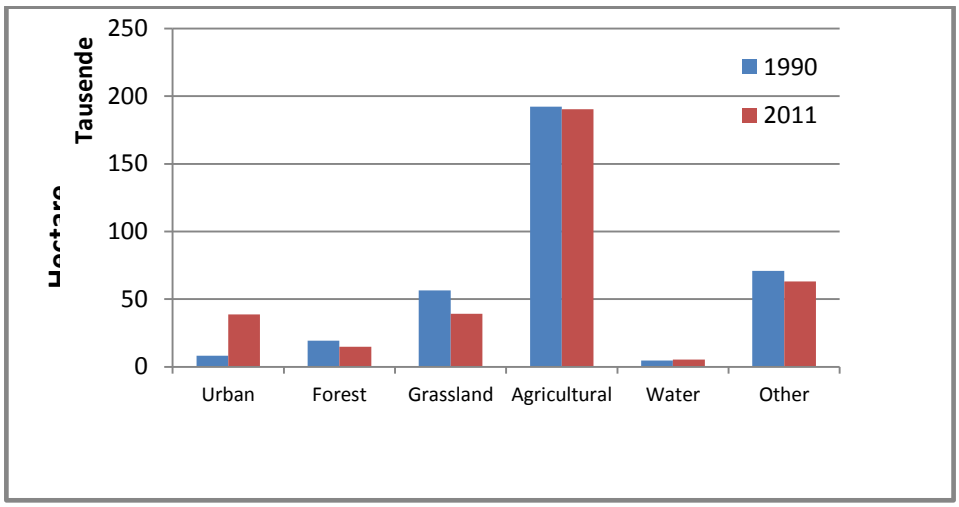

Figure 4.1. Show the percentage of the categories 1990 and 2011

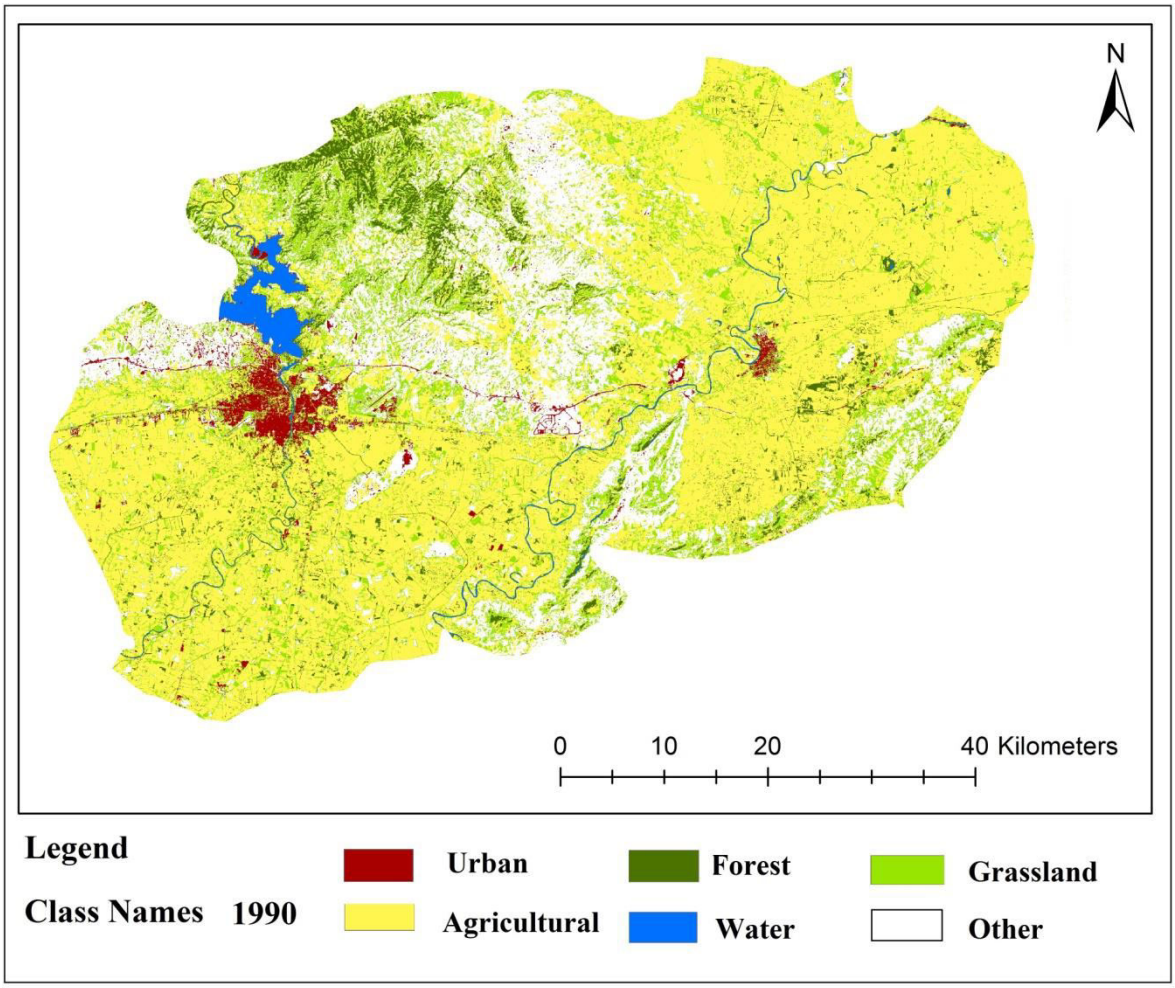

Figure 4.2. The Land Cover Classification Map of the 1990 TM Image

Table 4.1 Land Cover Types with their Corresponding Area (ha)

Land Cover Class	1990		2011	
	Area (ha)	Area (%)	Area (ha)	Area (%)
Urban	8213.49	2.33	38750.04	11.02
Forest	19277.82	5.48	14844.33	4.22
Grassland	56368.89	16.03	39106.62	11.12
Agricultural	192223.89	54.67	190451.97	54.17
Water	4632.75	1.31	5402.97	1.53
Other	70845.75	20.15	63006.66	17.92
Total	351562.59	100	351562.59	100

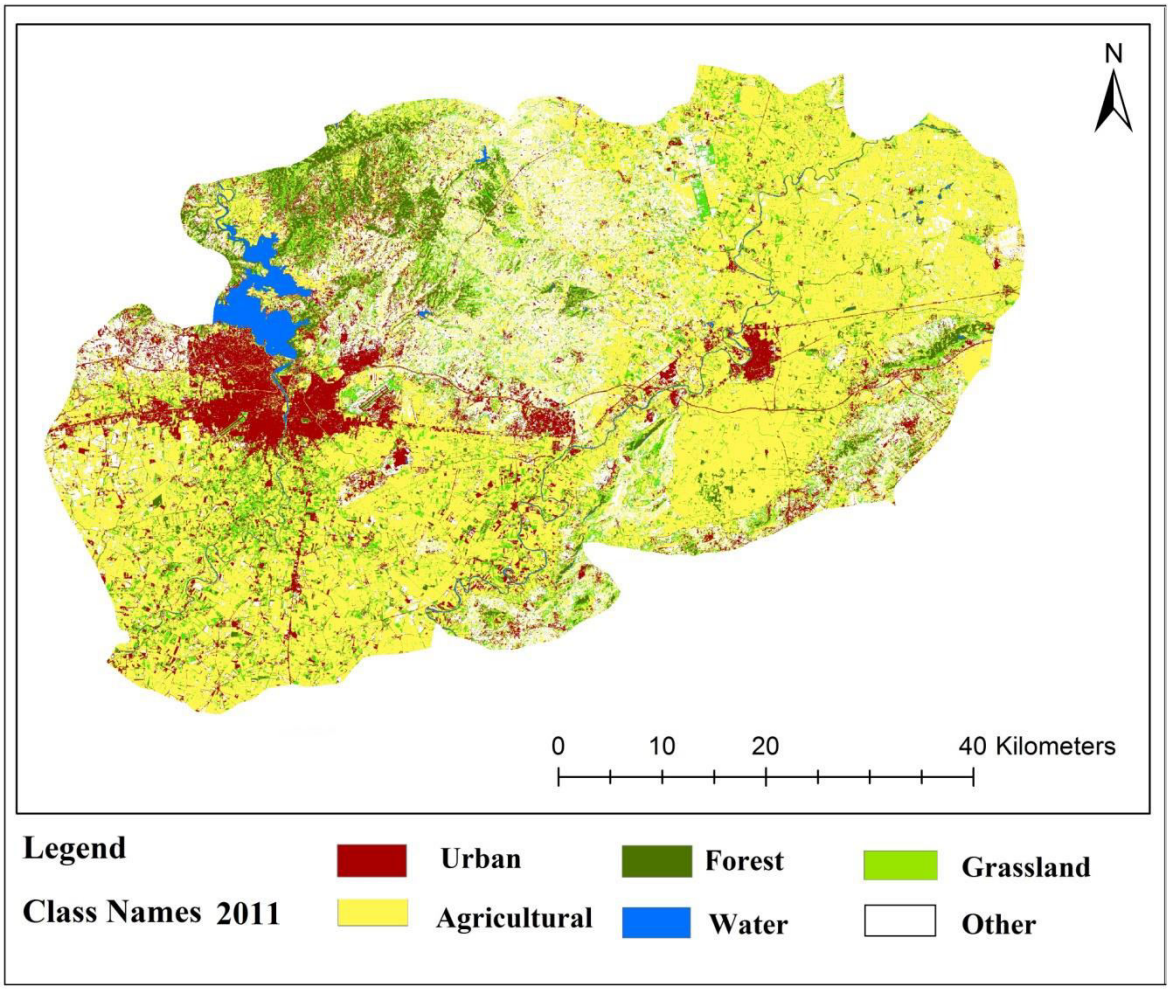

Figure 4.3. The Land Cover Classification Map of the 2011 TM Image

4.2. Accuracy Assessment

After the classification images, obtained LU/LC classes are controlled with accuracy assessment operation. One of the most common methods of classification accuracy assessment is error matrix or confusion matrix. Overall accuracy is measured in percent and represents the number of pixels correctly classified divided by the total number of pixels (Bobrinskaya, 2012).

During the accuracy assessment operation, randomly selected 180 random points for each image 1990 and 2011 separately to assess the success rate of classification result. Figure 4.4 and 4.5 show the accuracy assessment points. The overall accuracy LU/LC Classification was determined is 91.67% in 1990 and 93.33% in 2011. It is also, the kappa Statistics is 0.8823 in 1990 and 0.9056 2011. At the same time, user accuracy was found to be 87.27% for the 1990, 88.03% for 2011satellite data. As well as, Producers accuracy

showed that the 84.24% and 88.39 respectively. Summing up, table 4.2 and 4.3 showing the percentage of error confusion matrixes misclassified pixels for 1990 and 2011.

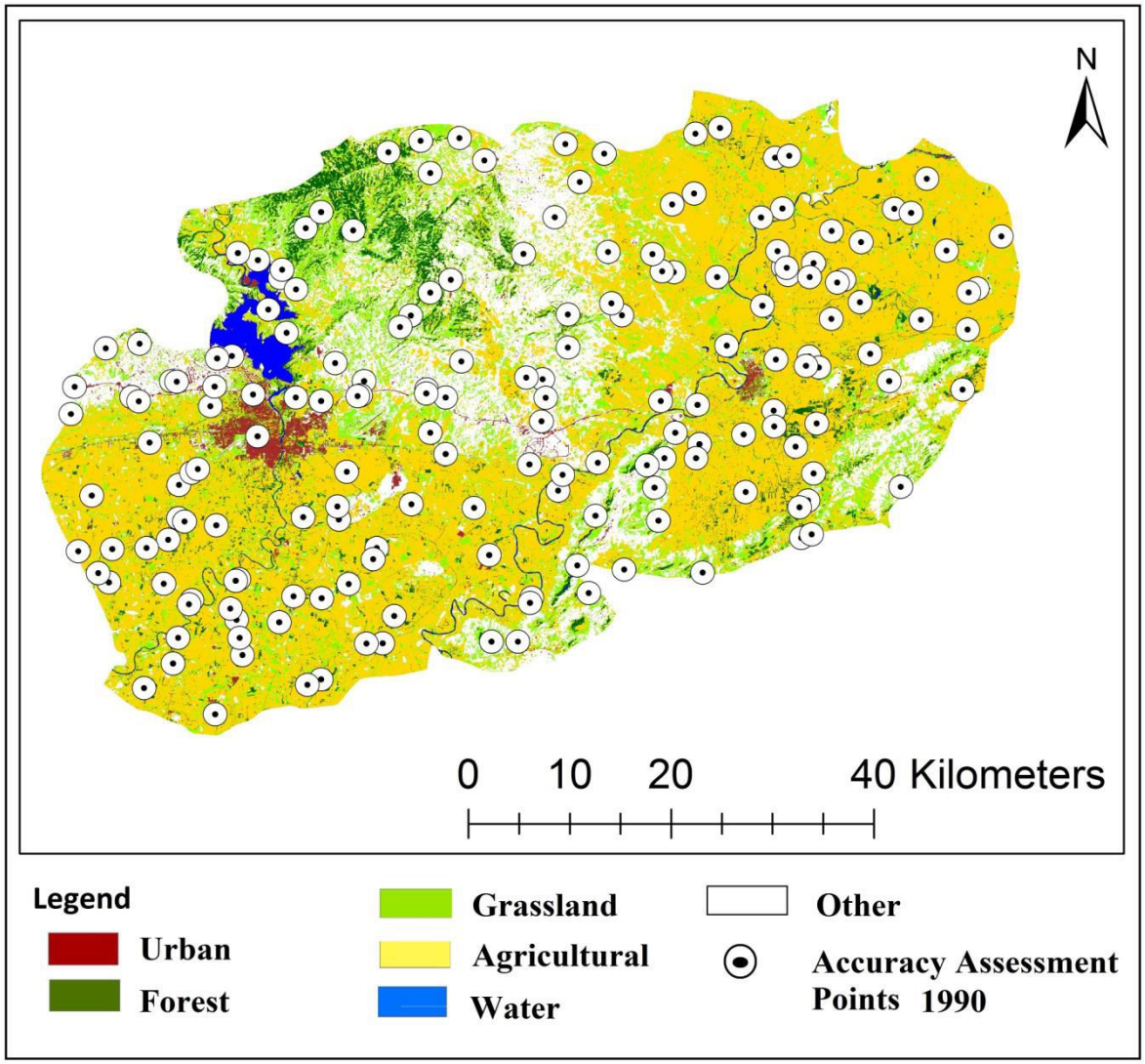

Figure 4.4. Showing the accuracy assessment points for the year1990

Table 4.2. Showing the percentage of error matrixes pixels for 1990

Class	Urban	Forest	Grass-Land	Agri-Cultural	Water	Other	Line Total	Producers accuracy %	Users accuracy %
Urban	35	0	0	1	0	0	36	66.67	92.31
Forest	0	25	4	1	0	0	30	82.35	73.68
Grassland	1	0	29	1	0	0	31	77.43	83.33
Agricultural	1	0	0	46	0	1	48	81.25	92.86
Water	0	0	0	0	12	0	12	100	100
Other	1	0	0	2	0	20	23	97.78	81.48
Total Column	38	25	33	51	12	21	180	84.24	87.27
Overall Classification Accuracy = 91.67%									
Overall Kappa Statistics = 0.88									(1990)

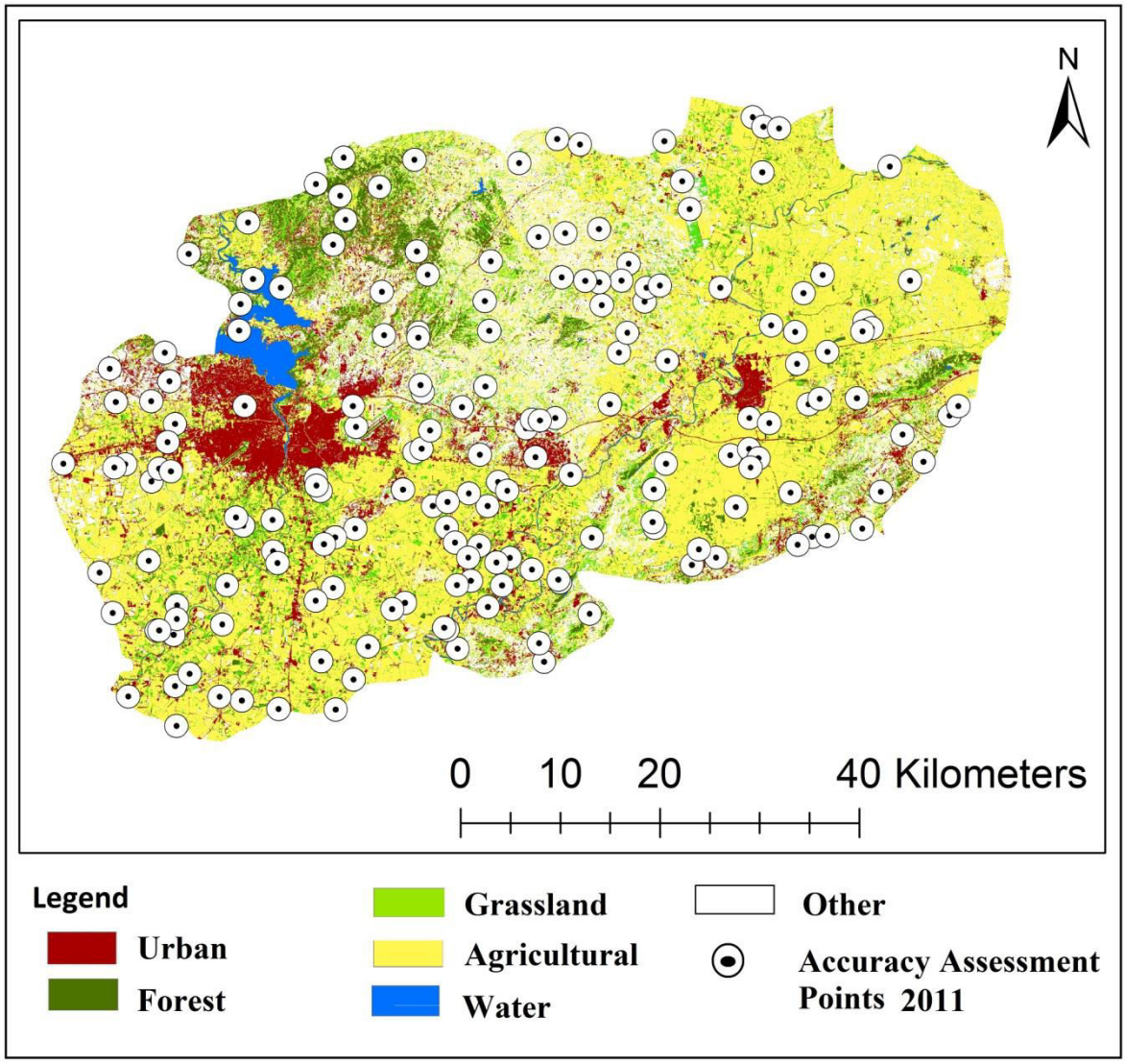

Figure 4.5. Showing the accuracy assessment points for the year 2011

Table 4.3. Showing the percentage of error matrixes pixels for 2011

Class	Urban	Forest	Grass-Land	Agri-cultural	Water	Other	Line Total	Producers accuracy %	Users accuracy %
Urban	32	0	0	0	0	2	34	83.33	68.18
Forest	0	20	3	3	0	0	26	80	80
Grassland	2	0	23	2	0	0	27	76.67	92
Agricultural	1	0	0	42	0	2	45	100	100
Water	0	0	0	0	14	0	14	100	100
Other	3	0	3	0	0	28	34	90.38	88
Total Column	38	20	29	47	14	32	180	88.39	88.03
Overall Classification Accuracy = 93.33%									
Overall Kappa Statistics = 0.90									(2011)

4.3. Change Detection

The change map and the transition matrix generated provide information on the correlation between the categories transition. Thus, the difference in the image represents the difference between a land cover class in the 1990 and corresponding class in the 2011. Figure 4.6 is a change map that shows the land cover changes were occurred between the six cover classes.

Moreover, the table 4.4 shows that, in 1990, urban area was covering of 8213.49 ha, 2.33%. Then increased to 38750.04 ha, 11.02% in 2011. It meant increased about 8.69% from 1990 to 2011. Usually, urban areas increasing in the passage of time who appear in other researches. For example: (Angel *et al*., 2005), (Rahman *et al.,* 2011), (wang, 2012), (Weng, 2001).

By other types showed that, the area covered with water also increased from 4632.75 ha, 1.31% in 1990 to 5402.97 ha, 1.53% in 2011. In the table can be observed that there was a decrease of 19277.82 ha to 14844.33ha, 56368.89 ha to 39106.62 ha, 192223.89 ha to 190451.97 ha, 70845.75 ha to 63006.66 ha in Forest land, Grassland, Agricultural, and Other land respectively.

For the most part, the greatest difference that occurred within the period was a reduction in urban area. As well as, It can be observed from the table that 16609.23 ha urban land, 7850.97ha Forest, 14750.28 ha Grassland, 29732 ha Agricultural, 3898.98 ha Water and 77099.67 ha of other land respectively remained unchanged within the 1990-2011 period.

Therefore, it can be inferred that the amount of change for the 1990-2011 period was 28.92%. Usually, the major land-use change is caused by the increasing demand for non-urban land because of urban and manufacturing development. Also, this land use increase extends both to urban and rural areas.

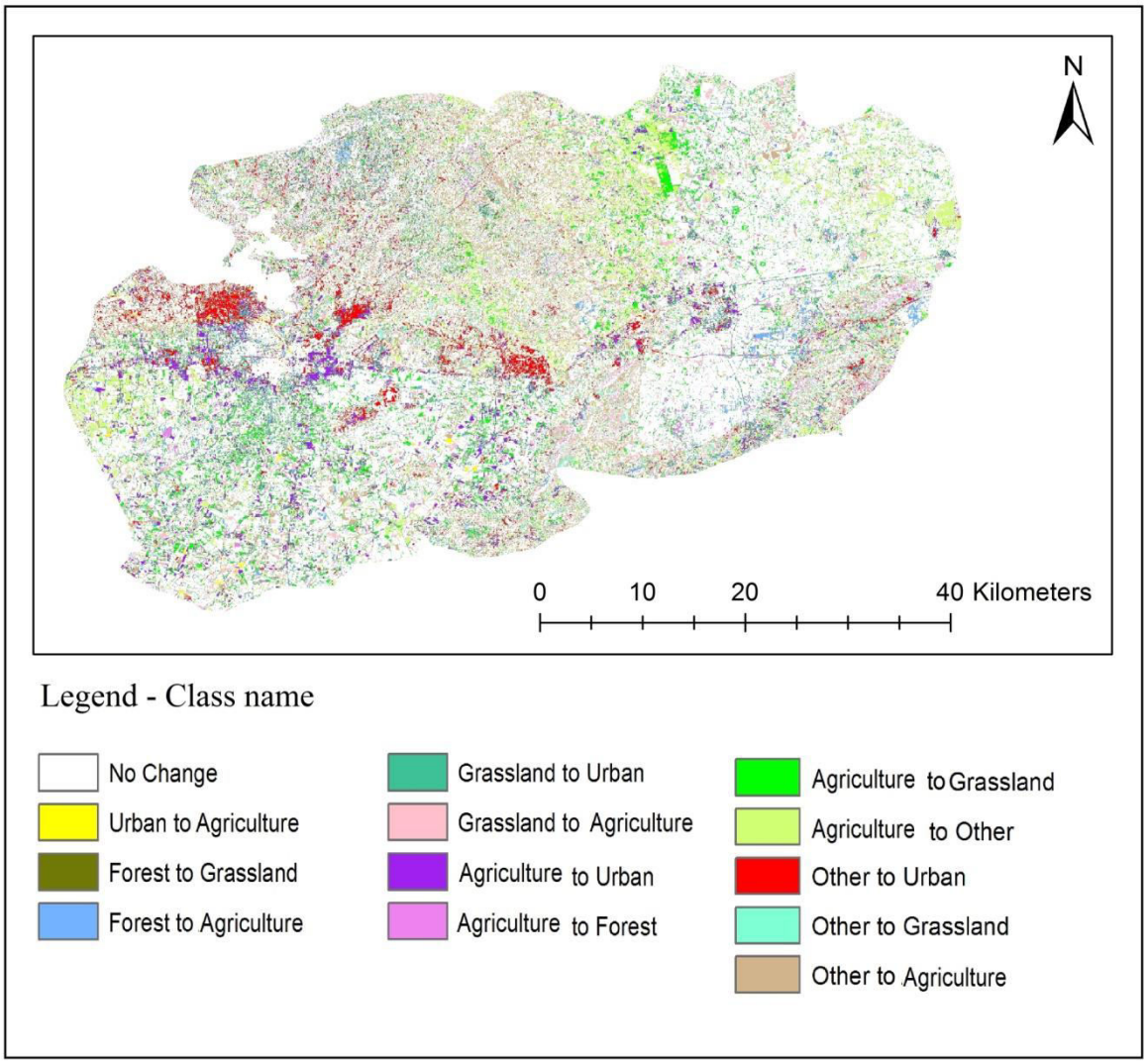

Figure 4.6. Change map showing Land Cover transition 1990 to 2011

Table 4.4. Land covers change detection1990-2011 (ha)

	LU/LC 1990						
LU/LC (ha) 2011	Urban	Forest	Grassland	Agricultural	Water	Other	Class total
Urban	16609.23	863.19	8626.41	1902.15	111.15	6291.09	34403.22
Forest	5187.24	7850.97	13416.93	3053.43	21.42	6148.8	35678.79
Grassland	5873.58	1961.64	14750.28	11291.85	122.85	9455.4	43455.6
Agricultural	10592.1	2059.47	26271.18	29732.04	18.99	29027.25	97701.03
Water	382.14	186.75	32.49	27.63	3898.98	201.06	4729.05
Other	20996.28	1215.09	23984.64	11925	374.22	77099.67	135594.9
Class Total	59640.57	14137.11	87081.93	57932.1	4547.61	128223.27	------
Change Class	43031.34	6286.14	72331.65	28200.06	648.63	51123.6	------
Image Difference	-25237.35	21541.68	-43626.33	39768.93	181.44	7371.63	------

4.4. Retrieving LST from RS Data

Based on (Oguz, 2013) in this study the single Chanel algorithm was used according to Radiance Transfer Equation (RTE) method. For there more, the various equations were used to calculation LST. The Land surface temperature was extracted from Landsat 5 TM image with thermal band 6 of the 1990 and 2011. The LST maps were produced to show the spatial distribution LST. Figure 4.7, 4.8, and 4.9 shows the spatial distribution of LST for each class in the study area.

The statistics of LST indicate that the temperature in the study area during the year 1990 was minimum 23.88°C and maximum 55.10°C, whereas in the year 2011 the minimum 23.34°C and maximum 59.03°C. In the table 4.5 can be obtained that, the mean temperature values of LU/LC classes increased from 1990 to 2011 while the mean temperature in 1990 is 27^{o}C then increase to 28^{o}C in 2011.

Overall, land surface temperature in 2011 is higher than in 1990, which can be seen in the figure 4.6, and 4.7. The result is similar with other researches such as: (Ahmed, *et al.,* 2013), (Jibril *et al*., 2012), (Ramachandra *et al*., 2012) who they investigate that, land surface temperature increasing between time periods. On the other hand, LST maps show that the land surface temperature for urban area is lower in 1990 than in 2011. The Mean land surface temperature of the "urban" class was 38.6 ^{o}C in 1990 their land surface temperature was 40 ^{o}C in 2011. Summing up, the mean temperature increased (1.4 ^{o}C) in the urban areas from 1990 to 2011.

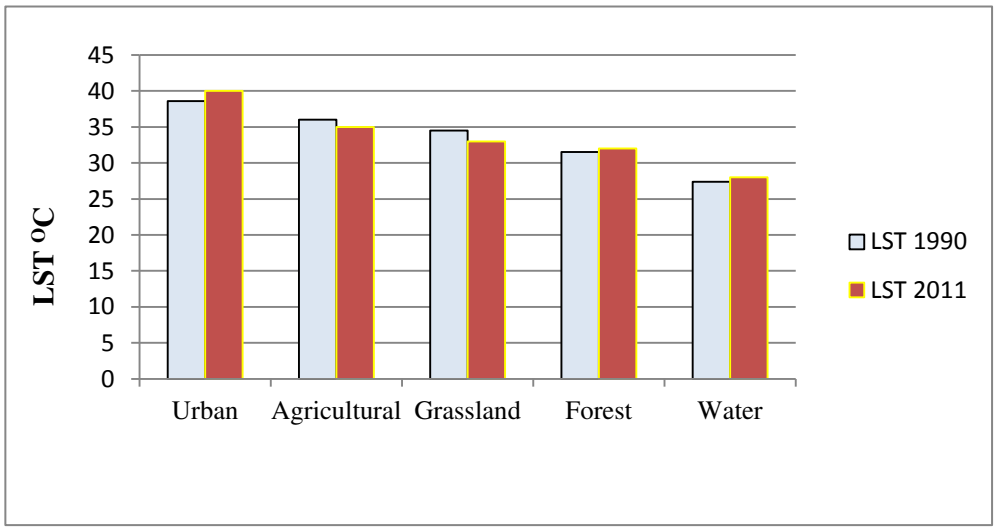

Figure 4.7. The deference LST according to LU/LC types 1990 – 2011

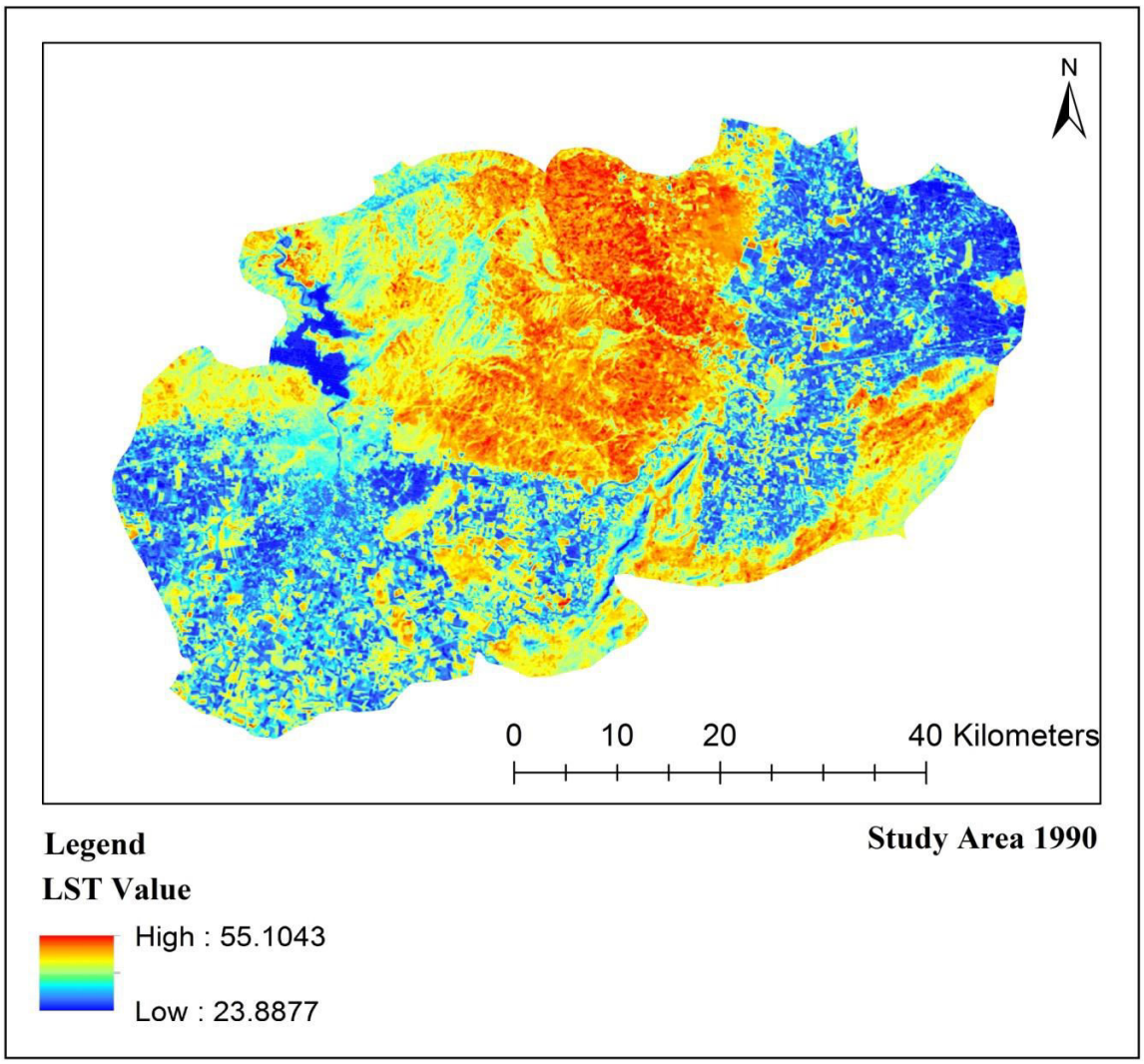

Figure 4.8. Map of Land Surface Temperature for 1990

Table 4.5. Land Surface Temperature in Degree Celsius 1990 - 2011

Class	LST 1990 ℃			LST 2011 ℃		
	Min	Max	Mean	Min	Max	Mean
Urban	23.88	58.66	38.6	23.42	57.29	40
Forest	23.90	49.21	31.5	23.89	50.10	32
Grassland	24.42	57.73	34	23.88	55.43	33
Agricultural	23.86	59.03	36	23.87	58.10	35
Water	23.85	46.32	27.4	23.86	45.16	28
Other	26.55	59.43	37	24.34	57.07	37.8

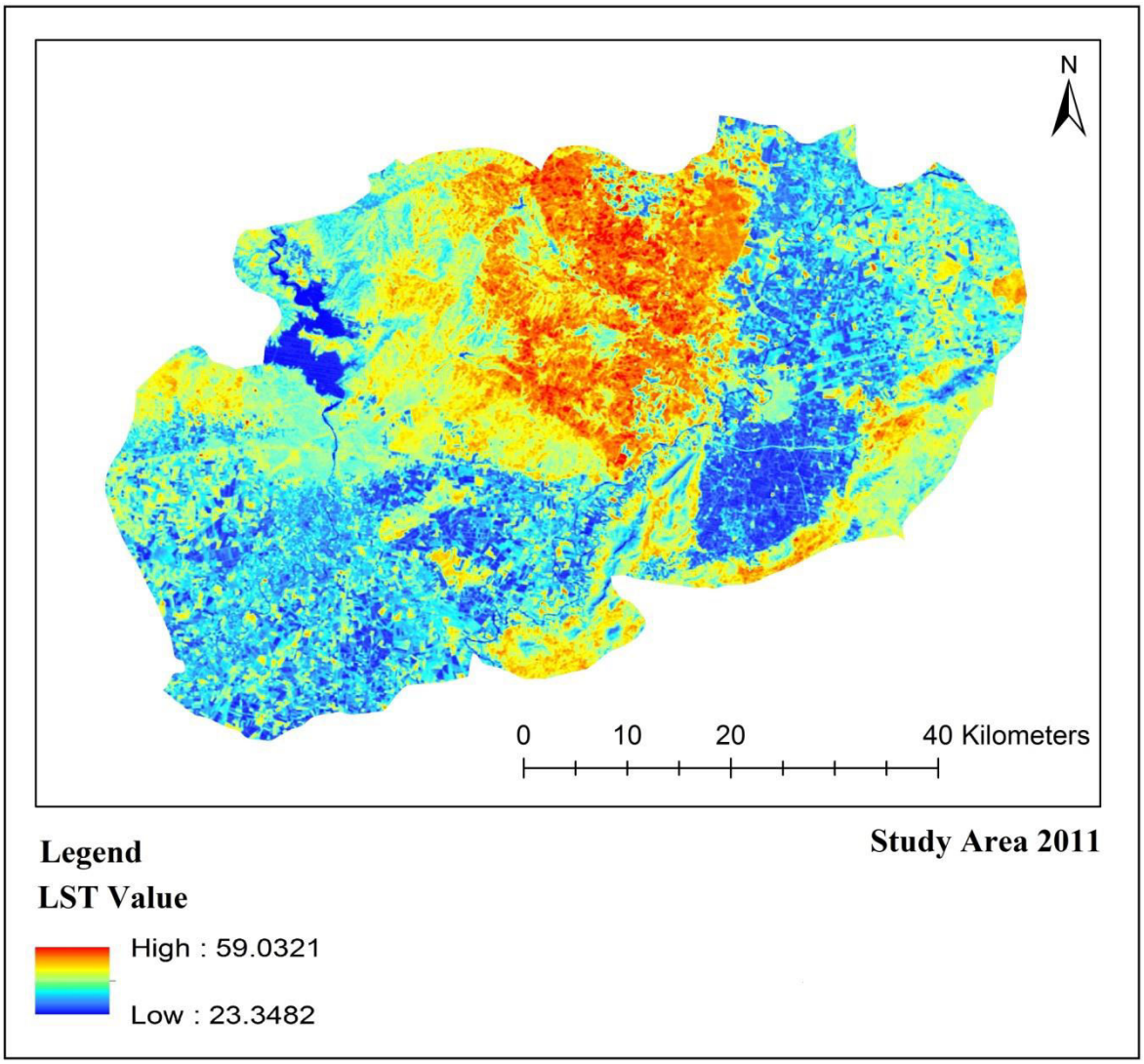

Figure 4.9. Map of Land Surface Temperature for 2011

4.5. Relationship between LU/LC and LST

The relationship between surface temperature and land cover types is shown in figures above. The urban areas have experienced maximum temperatures ranging between within 54.66 ℃ in 1990, and 57.29 ℃ in 2011. From LST maps it was observed that, the highest land surface temperature values in both years were recorded in "Urban" areas 38.6℃ in 1990 and 40℃ in 2011, whiles the lowest surface radiant temperature recorded in water 27.4 °C in 1990 and 28 °C in 2011.

In the table 4.5 can be observed that, the four land cover types (Urban, Forest, water, and other) have increase in surface temperature during the 21 years. The causes of increasing LST in urban areas suppose that, the concrete, stone, metal and asphalt are causes for make land surface temperature to rise. It is obvious that, population growth and

the rapid development of the urbanization have an extreme impact on the increase land surface temperature. On the other hand, a lot of building is one of the factors raise the land surface temperature in urban area.

The present findings seem to be consistent with other research of (Buyadi *et al*., 2013) which indicated that, the implication of urban development by replacing natural vegetation (forest) to built-up surfaces such as concrete, stone, metal and asphalt clearly can increase the surface radiant temperature. In other words (Mbithi *et al.,* 2010) say that, the conversion of forest and agricultural land into urban/built-up land is cause of contributed to the increased LST. Furthermore, the conversion of forest and agricultural land into urban/built-up land also contributed to the increased LST, while vegetation has great impact on reducing land surface temperature. Those causes obtained in some researches, for instance: (stemn, 2013), (Weng, 2001), (Mbithi *et al*., 2010).

On the theme of urban land, the land surface temperature is higher than Agricultural and Grassland. The Urban land exhibited the highest LST. It is reasonable, because the images were recorded at the morning as we know that the components of urban areas are receive sunbeam at the day then Reduce at night. Therefore, if the corresponding satellite images are recording at night the results will be change.

4.6. Relationship between NDVI and LST

The NDVI map generated for the study area1990 and 2011. Therefore, the relationship between NDVI and radiant surface temperature for each of the images was investigated through correlation analysis (pixel by pixel). Figures 4.10 and 4.11 are a maps that shows the NDVI values for the study area images. The Relationship between NDVI and Land Surface Temperature is shown that the NDVI negatively correlate with radiant surface temperature.

In other words, it means that where NDVI is lower have higher land surface temperature and where NDVI is higher have lower land surface temperature. Meanwhile, (Bobrinskaya, 2012) say that these negative values show that the temperatures are higher where there is no vegetation or the vegetation is weak.

Based on (Weng *et al*., 2004), LST is negatively correlated with green vegetation pixel fraction and positively correlated with impervious surface percentage.

The correlation between NDVI and LST is depicted in figure 4.12, and 4.13. It can be observed in Tables 4.6 and 4.7 that there is a negative Pearson's correlation between NDVI and surface temperature for two images. The range of NDVI is showed that, -0.006 to 0.694 in 1990, and -0.002 to 0.698 in 2011. As well as, the result showed that, correlation is -0.84 Also, R^2 is 0.728 in 1990. While, correlation is -0.85, R^2 is 0.726 in 2011. At the same time minimum temperature value is 30.12, maximum is 48.75 in 1990. Also, minimum value is showed 32.22, maximum is 50.62 in 2011.

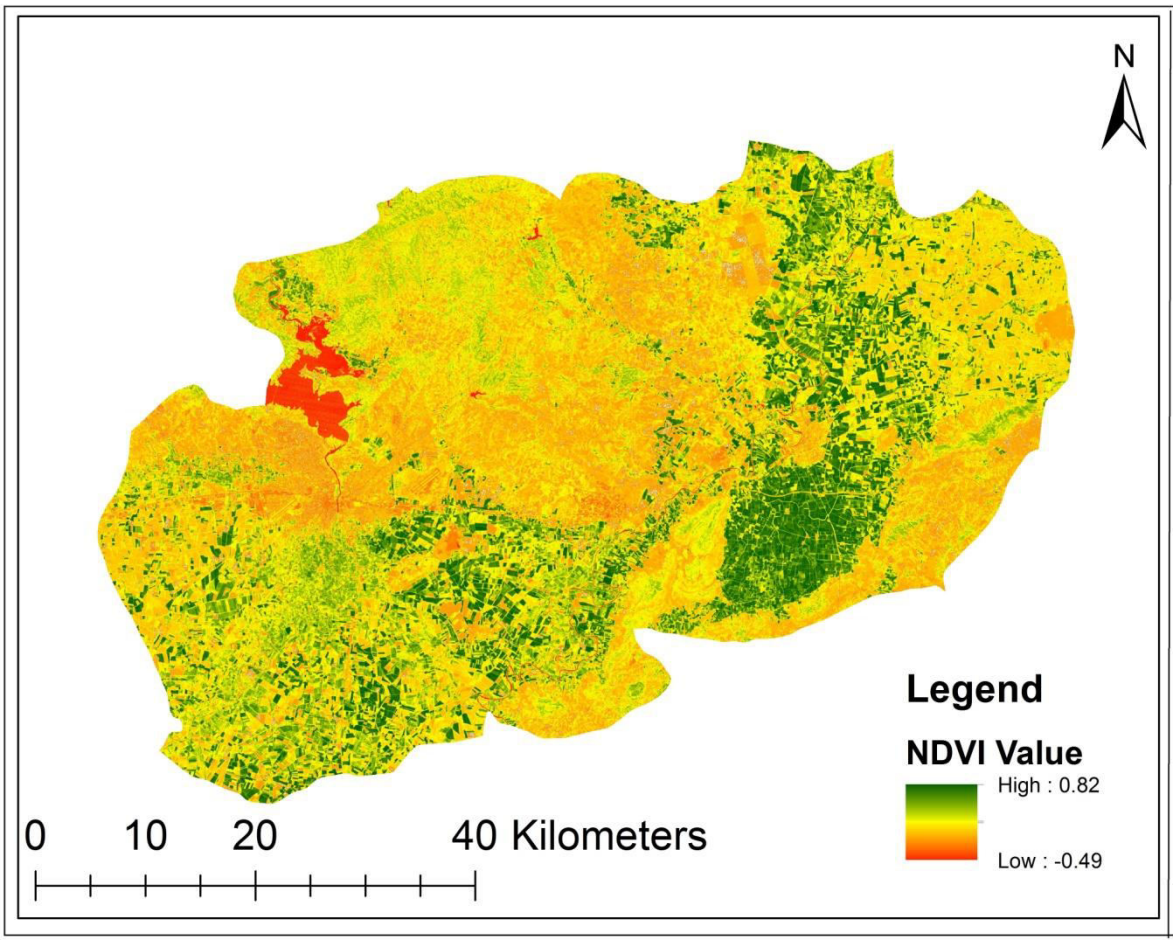

Figure 4.10. Map of NDVI for 1990

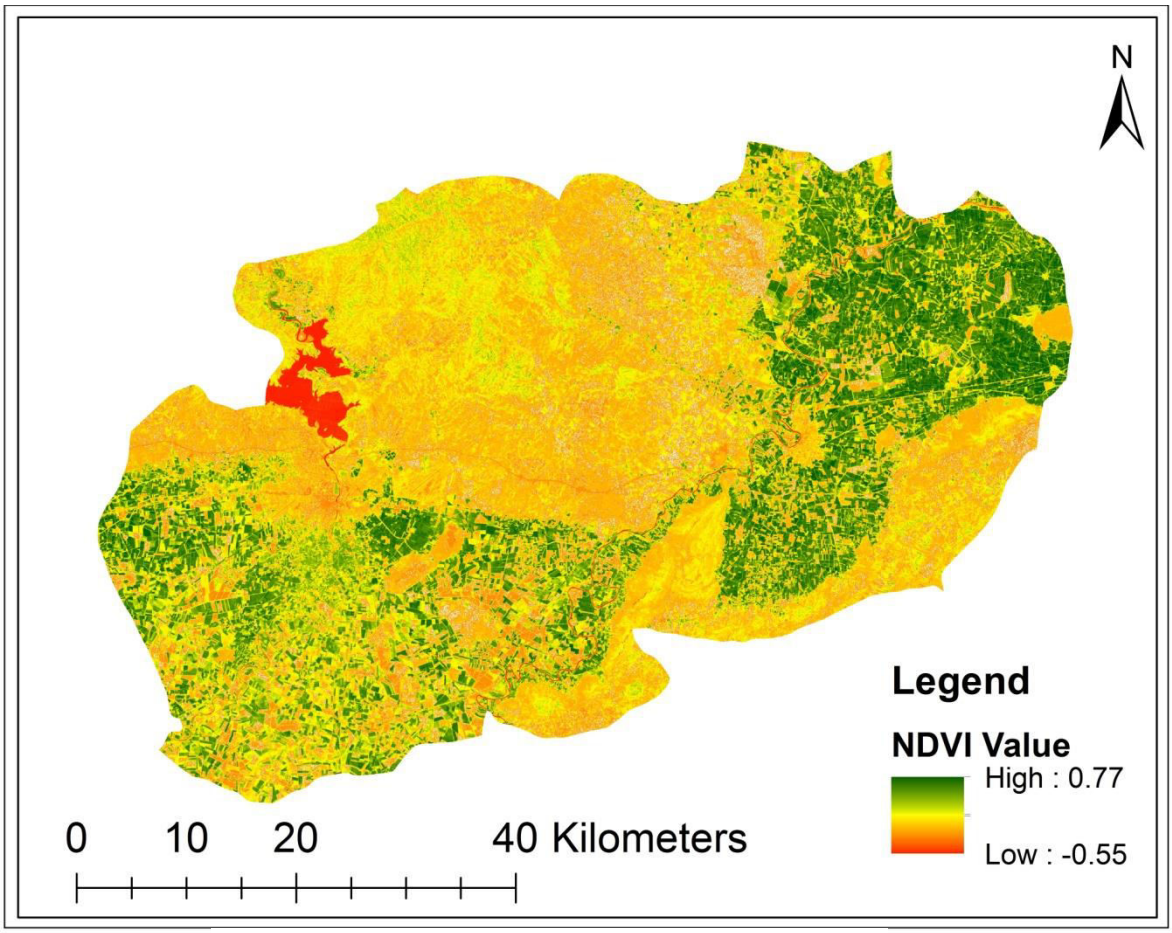

Figure 4.11. Map of NDVI for 2011

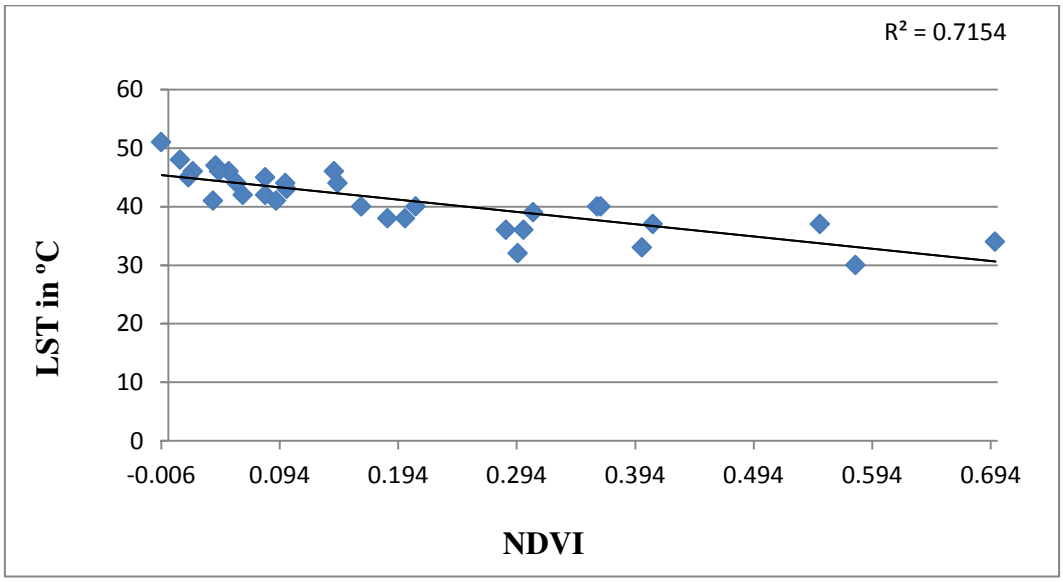

Figure 4.12. Relationships between NDVI and LST 1990

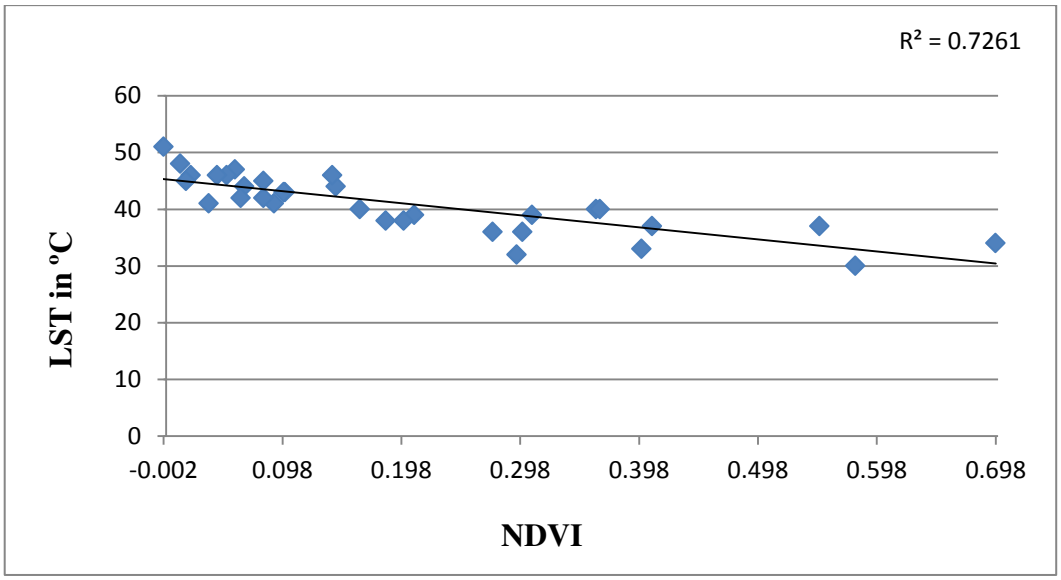

Figure 4.13. Relationships between NDVI and LST 2011

Table 4.6. Pearson's Correlation Coefficient between NDVI and Surface Temperature 1990

Relationship between NDVI and LST 1990									
No	X	Y	NDVI	LST	No	X	Y	NDVI	LST
1	717352.808	4112160.388	0.038	41	21	747292.808	4126500.388	0.308	39
2	688792.808	4103940.388	0.100	43	22	714112.808	4118250.388	0.295	32
3	775642.808	4118520.388	0.285	36	23	737392.808	4123500.388	0.365	40
4	727912.808	4072770.388	0.021	46	24	696052.808	4106100.388	0.185	38
5	690922.808	4091430.388	0.300	36	25	767332.808	4077930.388	0.209	40
6	760822.808	4076670.388	0.200	38	26	768442.808	4106670.388	0.040	47
7	748612.808	4079310.388	0.017	45	27	768142.808	4106370.388	0.082	42
8	767332.808	4090770.388	0.580	30	28	689092.808	4105170.388	-0.006	51
9	758872.808	4080000.388	0.550	37	29	733312.808	4112610.388	0.063	42
10	702472.808	4102800.388	-0.124	48	30	753832.808	4086960.388	0.409	37
11	774982.808	4127250.388	-0.123	47	31	747442.808	4104870.388	0.698	34
12	700132.808	4119750.388	0.051	46	32	755512.808	4103280.388	-0.057	46
13	722872.808	4081800.388	-0.090	52	33	692032.808	4114770.388	0.099	44
14	688942.808	4118400.388	0.091	41	34	775252.808	4094040.388	0.043	46
15	703462.808	4119390.388	0.010	48	35	694792.808	4103070.388	-0.124	51
16	734212.808	4127250.388	-0.026	47	36	748282.808	4098150.388	0.082	45
17	746002.808	4100430.388	0.140	46	37	716212.808	4104480.388	-0.125	51
18	686812.808	4114800.388	0.362	40	38	740572.808	4087980.388	0.400	33
19	763072.808	4124610.388	-0.510	49	39	742192.808	4099830.388	0.143	44
20	764962.808	4080000.388	0.058	44	40	762142.808	4120830.388	0.163	40
Correlation = -0.84									

Table 4.7. Pearson's Correlation Coefficient between NDVI and Surface Temperature 2011

Relationship between NDVI and LST 2011									
No	X	Y	NDVI	LST	No	X	Y	NDVI	LST
1	723952.8085	4093830.388	0.580	30	21	774262.8085	4129620.388	0.209	39
2	729262.8085	4114860.388	0.091	41	22	689932.8085	4096170.388	0.021	46
3	691672.8085	4103940.388	0.550	37	23	691612.8085	4084350.388	0.409	37
4	715252.8085	4093500.388	0.362	40	24	753682.8085	4086360.388	0.300	36
5	753412.8085	4108260.388	-0.510	50	25	687622.8085	4097250.388	0.698	34
6	690142.8085	4089930.388	-0.123	47	26	696082.8085	4102890.388	0.051	46
7	741052.8085	4111890.388	-0.125	51	27	765682.8085	4095060.388	0.043	46
8	731092.8085	4115520.388	0.400	33	28	749272.8085	4087320.388	-0.100	52
9	727222.8085	4082760.388	0.036	41	29	758092.8085	4102680.388	-0.124	51
10	738562.8085	4094640.388	0.143	44	30	696052.8085	4129620.388	0.063	42
11	762262.8085	4103130.388	-0.124	48	31	740422.8085	4096170.388	0.200	38
12	758542.8085	4070910.388	0.163	40	32	774262.8085	4084350.388	-0.057	46
13	734872.8085	4082190.388	0.058	47	33	689932.8085	4086360.388	-0.026	47
14	759022.8085	4122150.388	0.082	42	34	691612.8085	4097250.388	0.099	43
15	689272.8085	4093830.388	0.100	43	35	753682.8085	4102890.388	0.140	46
16	693562.8085	4114860.388	0.082	45	36	687622.8085	4095060.388	0.295	32
17	774022.8085	4103940.388	0.066	44	37	696082.8085	4087320.388	0.365	40
18	709222.8085	4093500.388	0.308	39	38	765682.8085	4102680.388	0.017	45
19	700612.8085	4108260.388	0.275	36	39	749272.8085	4119240.388	0.012	48
20	707602.8085	4089930.388	0.185	38	40	758092.8085	4088340.388	-0.002	51
Correlation = -0.85									

5. CONCLUSION

In this study used the integration of remote sensing and GIS to identify LU/LC changes also to assess the impact on land surface temperature between the period of 1990 and 2011 in the city of Adana with surrounding areas. For this research, used Landsat 5 TM images of province of Adana acquired the 29, Aug 1990 and 23, Aug 2011 from (USGS) earth explorer website.

The LU/LC maps of the study area are developed by supervised classification of the images. A maximum likelihood classifier is applied on the satellite images to derive LU/LC classification. Six classes were identified (Urban, Forest, Grassland, Agricultural, Water, and Other). Overall Classification Accuracy for 1990 and 2011 are 91.67% and 93.33% respectively.

The result of change detection analysis showed that the urban area increased 7.18% during the 21 years period. And this subsequently has resulted in the loss of non-urban lands such as farmland, forestland and etc. The urban land in the study area increased from 8213.49 ha in 1990 to 38750.04 ha in 2011. This increase could be attributed to the accelerated economic growth and increase in human population over the last two decades.

On the other hand, the results show that from 1990 to 2011, Urban and Grassland had the largest land use change. Overall, the main increasing trend is for Urban. In this period, urban land and Water were increasing and all other LU/LC types were decreasing.

Through this analysis, the LU/LC changes was studied Meanwhile the corresponded LST for each land use were extracted. In this research, the single - channel method used to retrieve LST consist on applying the Radiative Transfer Equation from a Radiative Transfer Code as MODTRAN.

The result of the analysis of the land surface temperature in terms of land cover classification showed that urban land has the highest surface temperature values. As the mean temperature is 38.6^{o}C in 1990 and 40^{o}C in 2011. In the same period (Water) land has the lowest amount of LST that is 27.4^{o}C and 28^{o}C respectively.

The amount of LST for the study area has increased from 1990 to 2011 by 1.4 ◦C which could be due to LU/LC changes. Such as: Urban area increasing in 1990 to 2011, 8213.49 ha 38750.04 ha, and also possible variations in weather temperature.

Moreover, the abundance of forest was an important factor to influencing land surface temperature. It is also; urban area has first Sequence according to highest to lowest mean temperature with 38.6 ^{o}C in 1990 and 40 ^{o}C in 2011.

As realized that, urban development, quality of materials that use for buildings and roads causes an increase in surface temperature in urban area. In addition, the study showed that the change of surface temperature is dependent on NDVI and surface cover. Therefore, NDVI map for two Landsat images is extracted. The relationship between land surface temperature and NDVI is considered with respect of the difference in LU/LC.

Result of correlation analysis between the extracted land surface temperature and NDVI showed that the significant inverse correlation is -0.84 in 1990 and -0.85 in 2011. As well as, R. square obtained that 0.728 and 0.726 respectively.

Finally the integration of GIS and remote sensing has therefore demonstrated their effective and efficient approach of analyzing and monitoring urban expansion patterns and assessing its impact on land surface temperature.

REFERENCES

Alig, R. J., & Healy, R. G. 1987. Urban and built-up land area changes in the United States: an empirical investigation of determinants. Land Economics, 215-226.

Acharya, P. K., Robertson, D. C., & Berk, A. 1993. Upgraded line-of-sight geometry package and band model parameters for MODTRAN (No. SSI-TR-226). SPECTRAL SCIENCES INC BURLINGTON MA.

Tayanc, M., & TOROS, H. 1997. Urbanization effects on regional climate change in the case of four large cities of Turkey. Climatic Change, 35(4), 501-524.

Prata, F. 2000. The proposed global land surface temperature product for ENVISAT's AATSR: Scientific basis, algorithm description and validation protocol. In Abstract for ERS-ENVISAT Symposium (pp. 16-20).

Weng, Q. 2001. A remote sensing? GIS evaluation of urban expansion and its impact on surface temperature in the Zhujiang Delta, China. International journal of remote sensing, 22(10), 1999-2014.

Luck, M., & Wu, J. 2002. A gradient analysis of urban landscape pattern: a case study from the Phoenix metropolitan region, Arizona, USA. Landscape ecology, 17(4), 327-339.

Qin, Z., Karnieli, A., & Berliner, P. 2002. Remote sensing analysis of the land surface temperature anomaly in the sand-dune region across the Israel-Egypt border. International Journal of Remote Sensing, 23(19), 3991-4018.

Liang, S., Fang, H., Morisette, J. T., Chen, M., Shuey, C. J., Walthall, C., & Daughtry, C. S. 2002. Atmospheric correction of Landsat ETM+ land surface imagery. II. Validation and applications. Geoscience and Remote Sensing, IEEE Transactions on, 40(12), 2736-2746.

Vermote, E. F., El Saleous, N. Z., & Justice, C. O. 2002. Atmospheric correction of MODIS data in the visible to middle infrared: first results. Remote Sensing of Environment, 83(1), 97-111.

Sobrino, J. A., Jiménez-Muñoz, J. C., Labed-Nachbrand, J., & Nerry, F. 2002. Surface emissivity retrieval from digital airborne imaging spectrometer data.Journal of Geophysical Research: Atmospheres (1984–2012), 107(D23), ACL-24.

Gedik, A. 2003 Differential urbanization in Turkey: 1955-2000. InERSA conference papers (No. ersa03p335). European Regional Science Association.

Chander, G., & Markham, B. 2003 Revised Landsat-5 TM radiometric calibration procedures and postcalibration dynamic ranges. Geoscience and Remote Sensing, IEEE Transactions on, 41(11), 2674-2677.

Sobrino, J. A., Jiménez-Muñoz, J. C., & Paolini, L. 2004 Land surface temperature retrieval from LANDSAT TM 5. Remote Sensing of environment,90(4), 434-440..

Weng, Q., Lu, D., & Schubring, J. 2004. Estimation of land surface temperature–vegetation abundance relationship for urban heat island studies.Remote sensing of Environment, 89(4), 467-483.

Angel, S., Sheppard, S., Civco, D. L., Buckley, R., Chabaeva, A., Gitlin, L., ... & Perlin, M. 2005. The dynamics of global urban expansion (p. 205). Washington, DC: World Bank, Transport and Urban Development Department.

Van, T. T. 2005. Relationship between Surface Temperature and Land Cover Types Using Thermal Infrared Remote Sensing, in Case of HoChiMinh City. InThe Sixteenth Workshop of OMISAR on the Application of Satellite Data, Vietnam.

Oguz, H. 2005. Modeling urban growth and land use/land cover change in the Houston Metropolitan Area from 2002-2030 (Doctoral dissertation, Texas A&M University).

Martine, G., & Marshall, A. 2007. State of world population 2007: unleashing the potential of urban growth. In State of world population 2007: unleashing the potential of urban growth. UNFPA.

Yuan, F., & Bauer, M. E. 2007. Comparison of impervious surface area and normalized difference vegetation index as indicators of surface urban heat island effects in Landsat imagery. Remote Sensing of Environment, 106(3), 375-386.

Berberoglu, S., Evrendilek, F., Ozkan, C., & Donmez, C. 2007. Modeling forest productivity using Envisat MERIS data. Sensors, 7(10), 2115-2127.

Reis, S. 2008. Analyzing land use/land cover changes using remote sensing and GIS in Rize, North-East Turkey. Sensors, 8(10), 6188-6202.

Bazoglu, N. 2008. Cities in Transition: Demographics and the Development of Cities. Philadelphia: Pennsylvania State University.

Van, T. T., Trung, L. V., & Lan, H. T. 2009. Application of thermal remote sensing in study on surface temperature distribution of Ho Chi Minh city. In Spatial data serving people: land governance and the environment–building the capacity, 7th FIG regional conference, Hanoi, Vietnam (pp. 19-22).

Mbithi, D., Demessie, E,T,. Kashiri,T 2010. The impact of Land Use Land Cover (LULC) changes on Land Surface Temperature (LST); a case study of Addis Ababa City, Ethiopia. Kenya Meteorological Services, Laikipia Airbase,P.O. Box 192-10400 Nanyuki Town, Kenya

Hadjimitsis, D. G., Papadavid, G., Agapiou, A., Themistocleous, K., Hadjimitsis, M. G., Retalis, A., ... & Clayton, C. R. I. 2010. Atmospheric correction for satellite remotely sensed data intended for agricultural applications: impact on vegetation indices. Natural Hazards and Earth System Science, 10(1), 89-95.

Saleh, S. A. 2011. Impact of urban expansion on surface temperature in Baghdad, Iraq using remote sensing and GIS techniques. Canadian Journal on Environmental, Construction and Civil Engineering, Vol. 2, No. 8.

Ahmeda, B. M., Hataa, T., Tanakamarua, H., Abdelhadib, A. W., & Tadac, A. 2011. the spatial analysis of surface temperature and evapotranspiration for some land use/cover types in the gezira area, sudan.

Rahman, A., Kumar, Y., Fazal, S., & Bhaskaran, S. 2011. Urbanization and quality of urban environment using remote sensing and GIS techniques in East Delhi-India. Journal of Geographic Information System, 3(01), 62.

Azim,S,. Ashraful Islam, M.D 2011. Modeling for Estimating Land Surface Temperature form Landsat Thermal Imagery: A Case Study of New Delhi and Its Surrounding.

Bobrinskaya, M. 2012. Remote Sensing for Analysis of Relationships between Land cover and Land Surface Temperature in Ten Megacities. Master of Science thesis in Geoinformatics. Royal Institute of Technology (KTH), Stockholm, Sweden.

Köroğlu,T,. H, Jewell, Somik. Lall, Lozano,N, Gracia, and Hyoung, Wang. 2012. Turkey Urbanization Review.

Guo, Z. Wang, S.D., et al. 2012. Assess the effect of different degrees of urbanization on land surface temperature using remote sensing images. Procedia Environmental Sciences, 13, 935-942, doi:10.1016/j.proenv.2012.01.087.

Ramachandra, T. V., Aithal, B. H., & Sanna, D. 2012. Land Surface Temperature Analysis in an Urbanising Landscape through Multi-Resolution Data.

Omran, E. S. E. 2012. Detection of Land-Use and Surface Temperature Change at Different Resolutions.

Chima, C. I. 2012. Monitoring and modelling of urban land use in Abuja Nigeria, using geospatial information technologies.

Wang, X. 2012. Urban Sprawl and Sustainable Development in China.

Jibril,m.,bako,mm.,mb.,yunusa, kuta,gi,. , a, musa. 2012. An assessment of the impact of urban growth on land surface temperature in fct, Abuja using geospatial technique

Youneszadeh Jalili, S. 2013. The effect of land use on land surface temperature in the Netherlands. Lund University GEM thesis series.

Ogidiolu, A., Ifatimehin, O. O., & Abu, M. U. 2013. Land Use Change and Spatio Temporal Pattern of Land Surface Temperature of Nigeria's Federal Capital Territory. Centrepoint journal (Humanities Edition), 15(1).

Stemn, E. 2013. Assessment of Urban Expansion and Its Effect on Surface Temperature in the Sekondi-Takoradi Metropolis of Ghana–A Remote Sensing and GIS Approach (Doctoral dissertation).

Buyadi, S. N. A., Mohd, W. M. N. W., & Misni, A. 2013. Impact of Land Use Changes on the Surface Temperature Distribution of Area Surrounding the National Botanic Garden, Shah Alam. Procedia-Social and Behavioral Sciences, 101, 516-525.

Ahmed, B., Kamruzzaman, M., Zhu, X., Rahman, M. S., & Choi, K. 2013. Simulating land cover changes and their impacts on land surface temperature in Dhaka, Bangladesh. Remote Sensing, 5(11), 5969-5998.

Oguz, H. 2013. LST calculator: a program for retrieving land surface temperature from Landsat TM/ETM+ imagery. Environmental Engineering and Management Journal, 12(3), 549-555.

Akin, A., Erdogan, M. A., & Berberoglu, S. 2013. The Spatiotemporal Land use/Cover Change of Adana City. ISPRS-International Archives of the Photogrammetry, Remote Sensing and Spatial Information Sciences, 1(2), 1-6.

Kitiş, C. Ç., & Şenol, S. 2013. Determination and monitoring of land use changes by using quickbird satellite data and aerial photographs in a selected area of the Northern Adana in Turkey. EURASIAN JOURNAL OF SOIL SCIENCE, 2(2), 131-139.

Balçik, F. B. 2014. Determining the impact of urban components on land surface temperature of Istanbul by using remote sensing indices.Environmental monitoring and assessment, 186(2), 859-872.

Vahmani, P., & Hogue, T. S. 2014. High-resolution land surface modeling utilizing remote sensing parameters and the Noah UCM: a case study in the Los Angeles Basin. Hydrology and Earth System Sciences, 18(12), 4791-4806.

United Nations. Department of Economic and Social Affairs. World urbanization prospects: The 2014 revision. UN. ISBN 978-92-1-151517-6. ST/ESA/SER.A/352.

UNNGLS World Population 2013. URL (access date: 10.3.2015 http://www.un-ngls.org/spip.php?page=article_s&id_article=301

UN/HABITAT.2014. Housing & slum upgrading, URL (access date: 3.1.2015) http//unhabitat.orgurban-themeshousing-slum-upgrading

Geo/Copernicus, 2013. Monitoring urbanization from high resolution remote sensing data. URL (access date: 52.2015) http://gmes.gov.cz/en/article/monitoring-urbanization-high-resolution-remote-sensing-data in 1.2.2015.

Satimagingcorp.com. Satellite Imagery and GIS for Land Cover and Change Detection. URL (access date: 9.2.2015) http://www.satimagingcorp.com/applications/environmental-impact -studies/land_cover_and_change_detection/

ADANA.BTU, Adana a living city, URL (access date: 17.1.2015) http://intoff.adanabtu.edu.tr/images/kutuphane/1313city_life.pdf

Turkey.com, weather of Adana, URL (access date: 25.2.2015) http://turkey.com/akdeniz-regions/adana/

World Weather & climate.com, information, average weather in adana, turkey, URL (access date: 9.2.2015) http://www.weather-and-climate.com/average-monthly-Rainfall-Temperature-Sunshine,Adana,Turkey

climatemps.com. Adana Climate & Temperature. URL 9access date: 12.4.2015) http://www.adana.climatemps.com

WeatherSpark.com, Average Weather for Adana, Turkey. URL (access date: 2.4.2015) httpsweatherspark.comaverages32422Adana-Turkey

USGS. Landsat: A Global Land-Observing Program. USGS Fact Sheet 023-03 URL (access date: 12.1.2015) http://pubs.usgs.gov/fs/2003/0023/report.pdf

Intergraph, Handbook, erdas imagine 2014. URL (access date: 2.2.2015) http://download.intergraph.com/downloads/erdas-imagine-2014-%2864-bit%29?startdownload=1

ESRI, 2007. Handbook ,What Is GIS. URL (access date: 25.3.2015) http://www.co.rice.mn.us/sites/default/files/pdfs/maps/documents/WIGIS.pdf

The Yale Center for Earth Observation,2013. Converting Digital Numbers to Top of Atmosphere (ToA) Reflectance. URL (access date: 13.1.2015) ttp://www.yale.edu/ceo/Documentation/Landsat_DN_to_Reflectance.pdf

CURRICULUM VITAE

Personal information

Name : Soran Omar Ahmed

Nationality : Iraqi

Date and place of birth : 11/September/1983 Erbil, Iraq

Marital Status : Single

Email : Soran.ahmed2014@gmail.com

Phone Number : (+964) 750 456 1611

Education

Degree : B.Sc.

Department : Geography

College : College of Arts

University : Salahaddin University, Iraq

Publication

Hakan Oğuz, Soran Omar Ahmed, and Daban Kadhim Omer Dabbagh, 2015. "Adana Kent Büyümesinin Yer Yüzey Sıcaklığı Üzerine Etkisinin Belirlenmesi". Ecology, 2015, Symposium 6-9 May 2015, Sinop-Turkey. Poster presentations.